ORIGINAL PAPER

Initiation of the Unazuki Belt, Southwest Japan, during the Carboniferous as an island arc system along the North China Craton

Chang Whan Oh[1] · Kenta Kawaguchi[1,2,3] · Bo Young Lee[4] · Seung Hwan Lee[4] · Takeshi Imayama[5]

Abstract

The Unazuki Belt, Southwest Japan, is a part of the Hida Belt, which is characterized as a plutono-metamorphic complex with a continental affinity formed between the late Paleozoic and early Mesozoic. The Unazuki Belt is known to be an important tectonic unit for the tectonic correlation between the proto-Japan and East Asian continents as it records Permo–Triassic tectono-thermal events, however, comprehensive chronology of the Unazuki Belt including the timing of the initiation of this Belt is yet unclear. The present study reveals certain Carboniferous magmatic and sedimentation events from the Unazuki Belt and their tectonic implications for the first time as follows. Zircon U–Pb age dating results and whole-rock geochemical compositions show that the protoliths of metagranite and metatrachyandesite in the Unazuki Belt formed at 328.2 ± 4.4 Ma and 332.8 ± 2.2 Ma, respectively, in an arc tectonic setting. Most metasedimentary rocks of the Unazuki Belt have the youngest detrital zircon grains of ~ 300 Ma with the Carboniferous single cluster at ~ 340–300 Ma without any Pre-360 Ma detrital zircon grains. However, one metasedimentary rock with Precambrian detrital zircons ($\sim 20\%$) has the youngest detrital zircon age of ~ 252 Ma, and $\sim 66\%$ of detrital zircons show a Permian age. Most of the $\varepsilon_{Hf}(t)$ values of zircon grains from all the studied Unazuki Belt samples, including the metasedimentary and metaigneous rocks with Carboniferous ages (~ 360–300 Ma) are positive ($+6$–$+18$), whereas those of the zircon grains with Permian ages (~ 280–260 Ma) show wide variations between $+16$ and -23. The whole-rock geochemical compositions of the ~ 300 Ma metasedimentary rocks of the Unazuki Belt show an island arc tectonic setting, whereas those of ~ 252 Ma metasedimentary rock have a continental arc affinity. These new data suggest that (1) igneous and sedimentary rocks in the Unazuki Belt formed in the island arc tectonic setting separated from the margin of continental crust during the Carboniferous but shifted to the continental arc tectonic setting during the latest Permian, (2) the collision between the island arc and continental arc may have caused the intermediate-*P/T* metamorphism during the Permian in the Unazuki Belt. The Carboniferous island arc tectonic setting in the Unazuki Belt indicates that the Hida Belt, including the Unazuki Belt, formed not at the margin of the South China Craton where Carboniferous subduction is absent but on the continuous subduction zone located along the eastern margin of the North China Craton, including the eastern margin of the northern Korean Peninsula where Carboniferous subduction occurred.

✉ Kenta Kawaguchi
k-kawaguchi@hiroshima-u.ac.jp

[1] Department of Earth and Environmental Sciences, Jeonbuk National University, 567, Baekje-Daero, Deokjin-Gu, Jeonju 54896, Republic of Korea

[2] Division of Earth Sciences, Faculty of Social and Cultural Studies, Kyushu University, 744 Motooka, Nishi-Ku, Fukuoka 819-0395, Japan

[3] Transdisciplinary Science and Engineering Program, Graduate School of Advanced Science and Engineering, Hiroshima University, 1-7-1 Kagamiyama, Higashi-Hiroshima, Hiroshima 739-8521, Japan

[4] Geological Research Division, Korea Institute of Geoscience and Mineral Resources, Daejeon 34132, Republic of Korea

[5] Institute of Frontier Science and Technology, Okayama University of Science, 1-1 Ridai-Cho, Kita-Ku, Okayama 700-0005, Japan

Introduction

The Japanese Islands are considered to have been located on the eastern margin of the Asian continent, next to the Korean Peninsula, before the Miocene (e.g., Otofuji and Matsuda 1984; Maruyama et al. 1989; Otofuji 1996). Therefore, a correlative study of pre-Paleogene basement rocks between the Korean Peninsula and the Japanese Islands is important to understand the tectonic evolution of the eastern margin of East Asia (Matcalfe 2006; Oh 2006; Osanai et al. 2006; Oh and Kusky 2007; Dunkley et al. 2008). The tectonic correlation between the Korean Peninsula and Japanese Islands before the Miocene has been discussed in many studies (e.g., Ishiwatari and Tsujimori 2003; Oh 2006; Kawaguchi et al. 2023a, b), and different tectonic models have been proposed. In particular, the geological correlation before the Jurassic is quite uncertain due to the limited correlatable evidence.

The pre-Jurassic tectonic units in the Japanese Islands are widely exposed in the Inner Zone of Southwest Japan, which includes the Hida Belt, located on the most continental side of the Japanese Islands (Fig. 1). The rocks of the Hida Belt have a continental margin affinity, including the plutono-metamorphic complex that formed during the late Paleozoic to Mesozoic (e.g., Hiroi et al. 1978; Hiroi 1981, 1983; Kano 1990; Arakawa et al. 2000; Horie et al. 2010, 2013, 2018; Takahashi et al. 2010, 2018; Cho et al. 2021). The Hida Belt is further subdivided into the Unazuki Belt, Hida Metamorphic Belt, and Hida Granites, which intruded into both the Unazuki and Hida Metamorphic Belts (Fig. 2). An understanding of the pre-Jurassic tectono-thermal history and crustal evolution of the Hida Belt is important for the tectonic correlation between the East Asian continental margin, including the Korean Peninsula, and the Japanese Islands. The Hida Belt has long been believed to be part of the North China Craton (NCC) (Kobayashi 1941; Takahashi et al. 2018; Horie et al. 2010, 2018; Cho et al. 2021). However,
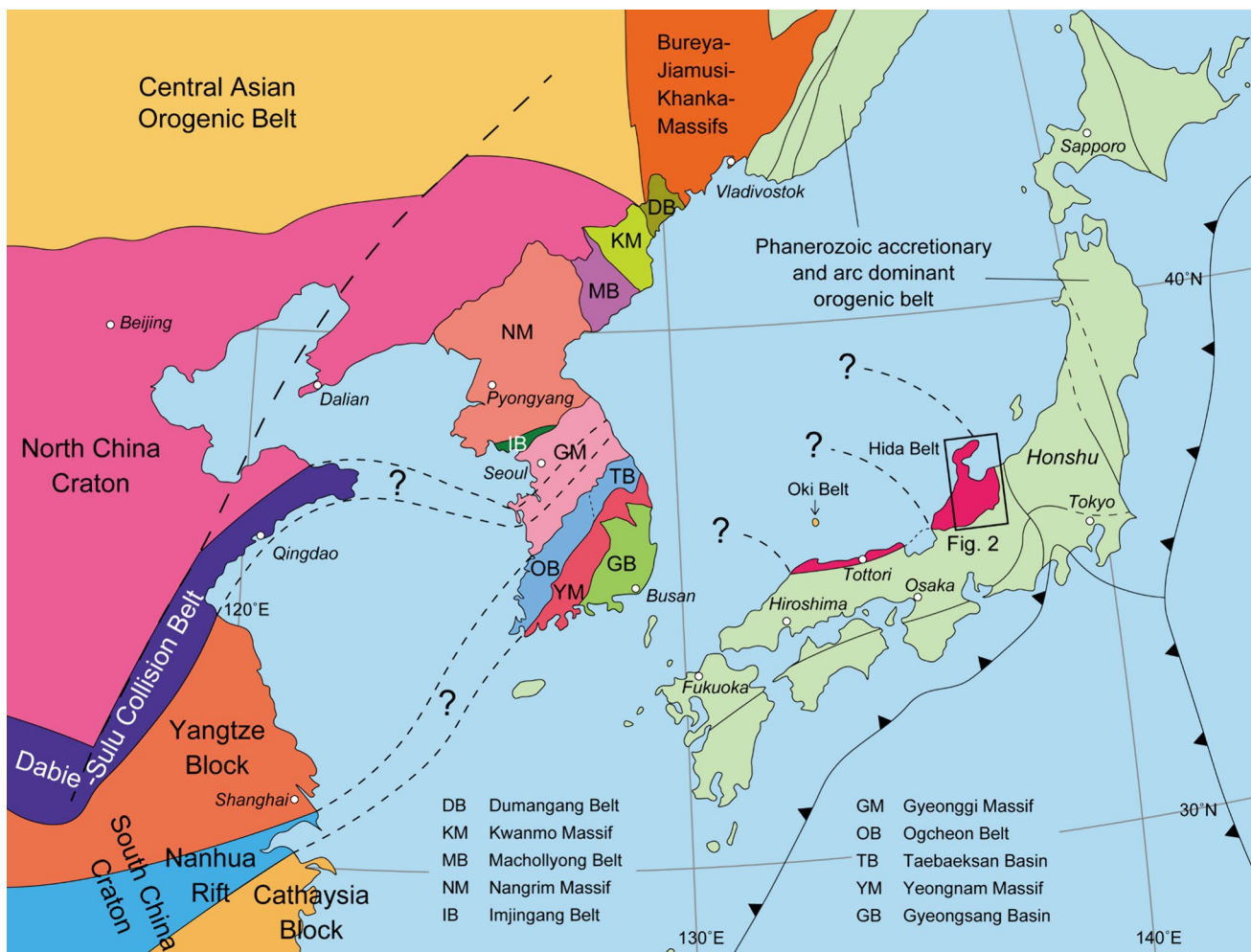

Fig. 1 Tectonic map of East Asia, including the Hida Belt, Southwest Japan
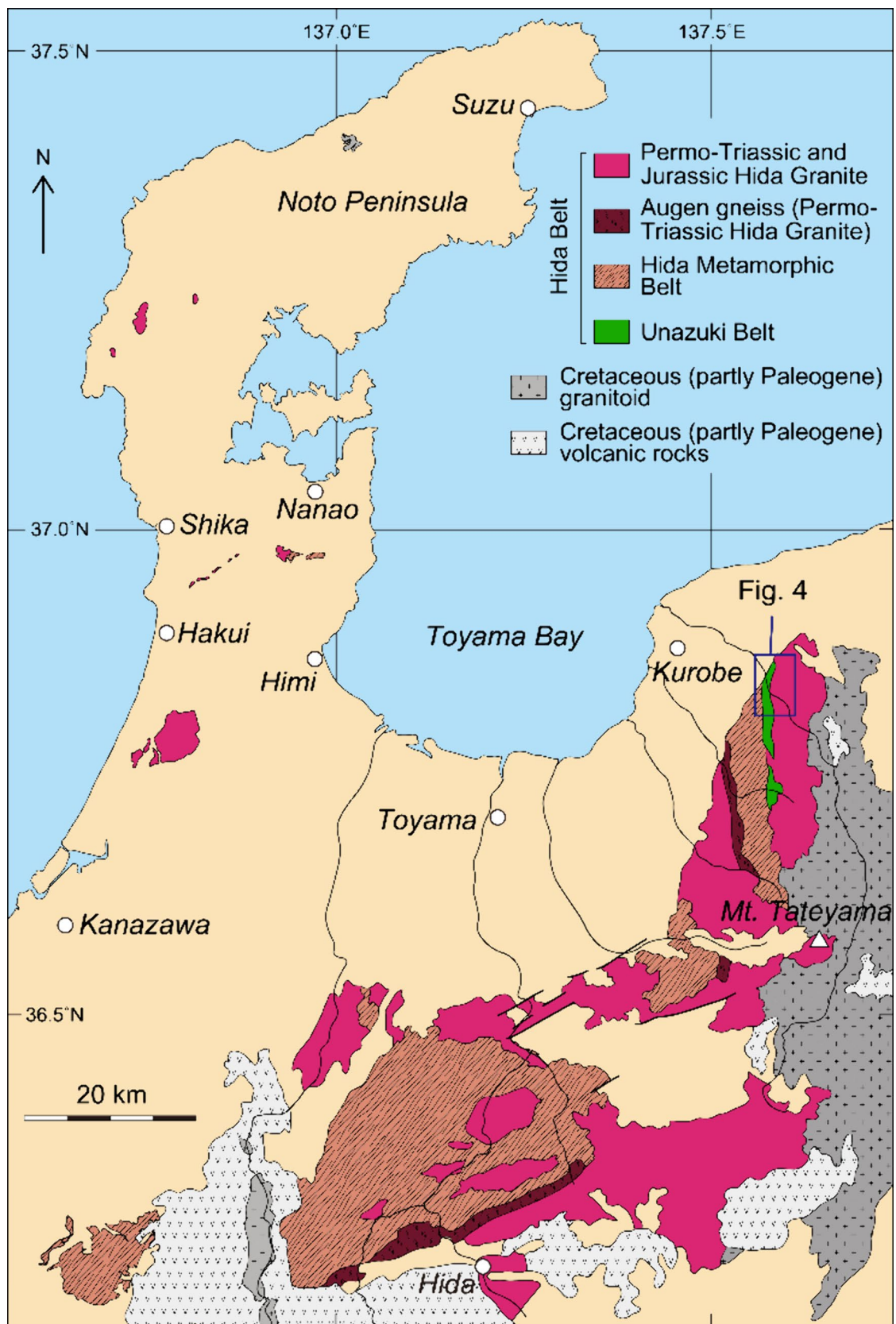
Fig. 2 Geological map of the Hida Belt including the Unazuki Belt area after Kano (1990). The mapped area is shown in Fig. 1

it was also suggested to be a part of the Jiamusi Massif, based on the similar age of igneous activities (Zhao et al. 2013) and the collision zone between the NCC and South China Craton (SCC), based mainly on the occurrences of the intermediate-pressure/temperature (*P/T*)-type metamorphic rocks (e.g., Sohma et al. 1990; Sohma and Kunugiza 1993). Some studies considered it to be a microcontinent that collided with the eastern edge of the NCC in the late Paleozoic (e.g., Mizutani and Hattori 1983; Ernst et al. 1988). This contrasting idea is mainly attributed to the limitation of the direct correlatable evidence between the Hida Belt and East Asian continental margins. Precambrian detrital/inherited zircon, including Archean ages, have been reported from the Hida Belt (Horie et al. 2010, 2018; Takahashi et al. 2018). However, based on previous studies thus far, the Hida Belt has been confirmed to consist of late Paleozoic to Jurassic rock units, and certain Precambrian rocks, which are major constituents of the NCC and SCC, have not been reported (e.g., Suzuki and Adachi 1991, 1994).

The origin and tectonic evolution of the Hida Belt are still uncertain, and particularly, the tectono-thermal events before ~ 260 Ma have not been well studied due to the limited lines of evidence (Fig. 3). The igneous ages older than 300 Ma were reported from the Hida Belt in previous studies, such as whole-rock Rb–Sr isochron ages of 415 ± 144 Ma (metagabbro) and 332 ± 74 Ma (metatonalite) (Arakawa

1984), whole-rock Rb–Sr model ages of ~ 1100 Ma (coarse-grained granite) and ~ 700 Ma (medium-grained granodiorite) (Shibata and Nozawa 1986), and Nd model ages of ~ 1500–1300 Ma (Shibata et al. 1989). However, the age dating methods used to obtain those ages have large uncertainties, and new chemical ages (~ 250–230 Ma) have been reported from the same body studied by Shibata and Nozawa (1986) using chemical Th–U–total Pb isochron method (CHIME) zircon and monazite dating (Suzuki and Adachi 1991). Moreover, Takeuchi et al. (2019) reported LA–ICP–MS zircon U–Pb ages of 241–229 Ma from the same outcrop studied by Shibata and Nozawa (1986). These contrasting results suggest that certain Precambrian rocks have not been reported thus far from the Hida Belt. A recent study revealed the important 302.2 ± 2.1 Ma magmatism from the orthogneiss in the Hida Metamorphic Belt based on the SHRIMP zircon U–Pb method (Fig. 3, Cho et al. 2021); however, its occurrence is very limited, and the comprehensive tectonic interpretation is still uncertain. Instead, almost all pre-300 Ma ages, including the Precambrian age in the Hida Belt, were obtained mainly from detrital/inherited zircon, and those data imply some pre-300 Ma tectono-thermal events in the Hida Belt (e.g., Takahashi et al. 2018). In particular, the Archean inherited zircon grains up to ~ 3.8 Ga were obtained from the ~ 256 Ma granites intruded in the Unazuki Belt (Horie et al. 2010, 2018), suggesting the
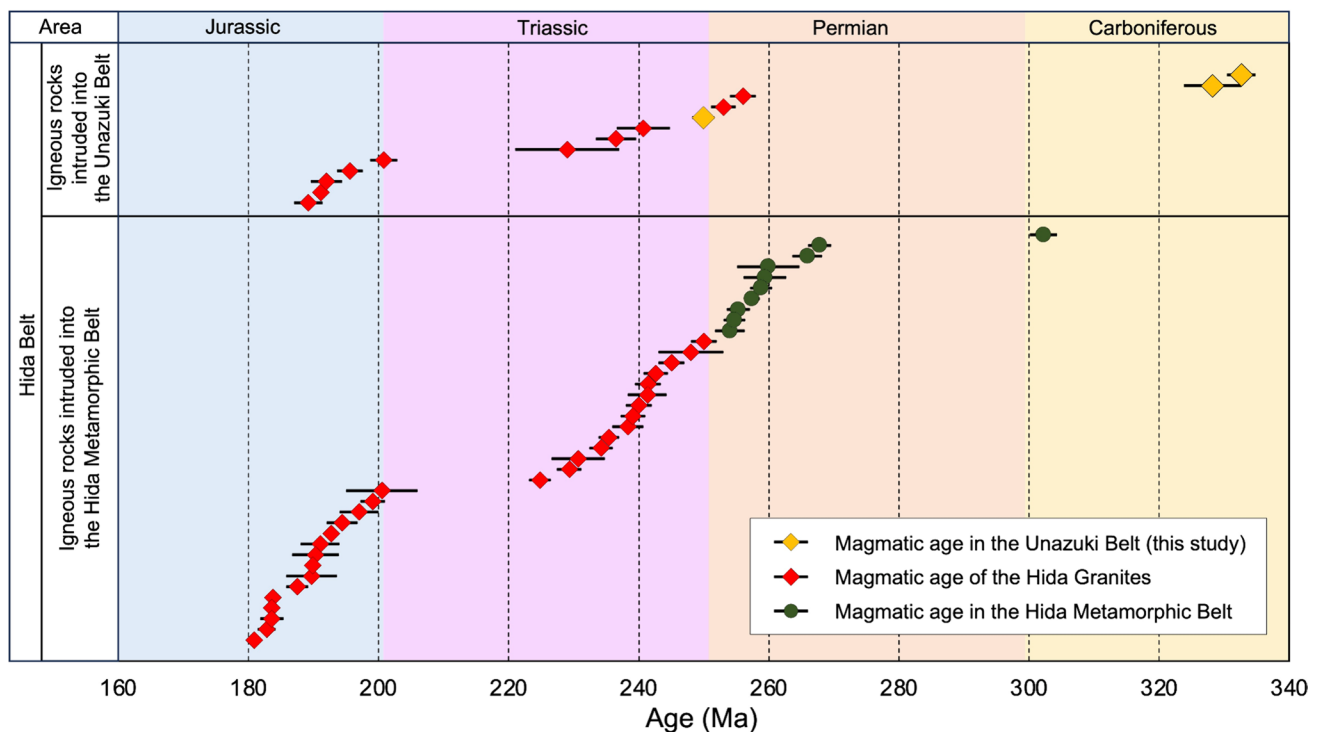

Fig. 3 Magmatic ages of the Hida Belt including the Unazuki Belt based on U–Pb zircon ages. Data are from Sakoda et al. (2006), Horie et al. (2010, 2013, 2018), Takahashi et al. (2010, 2018), Zhao et al. (2013), Koizumi and Otoh (2019), Takehara and Horie (2019), Takeuchi et al. (2019, 2021), Cho et al. (2021a), Yamada et al. (2021), Kawaguchi et al. (2023b) and this study

significant input of Archean crustal materials. However, pre-260 Ma tectono-thermal events are not fully understood due to the limited lines of evidence (Fig. 3).

Previously, there had been an active debate on the tectonic correlation between the Hida Belt and the East Asian continent, such as the correlation with the Ogcheon Metamorphic Belt in the southern Korean Peninsula (e.g., Hiroi 1981), the Dabie-Sulu collision belt between the NCC and SCC (Isozaki 1997; Arakawa et al. 2000), or the basements of the Korean Peninsula, including the Yeongnam, Gyeonggi, Nangrim, and Kwanmo Massifs and the Ogcheon Belt (e.g., Hiroi 1981; Isozaki 1997). However, these correlations are loosely constrained based on indirect and insufficient evidence without the quantitative data including the isotopic and petrochronological data. Therefore, to obtain a definitive correlational model, it is necessary to reexamine the characteristics of the Hida Belt based on reliable and high-resolution methods, such as zircon U–Pb dating and Lu–Hf isotope analysis coupled with petrological and geochemical investigations.

In the present study, LA–(MC–)ICP–MS zircon U–Pb age dating and Lu–Hf isotope analysis were carried out on samples from the Unazuki Belt to reveal the timing of magmatism and the age of deposition, with the characteristics of the source materials. Whole-rock geochemical analyses were also carried out for the samples from the Unazuki Belt to reveal their tectonic settings. In this study, we obtained important zircon U–Pb ages including ~330 Ma igneous and ~300 Ma sedimentation ages from the Unazuki Belt for the first time, and the detailed investigations provided in this study play a pivotal role in revealing the pre-300 Ma tectono-thermal evolution of the Unazuki Belt. Finally, the tectonic correlation between the Hida Belt including the Unazuki Belt, and East Asia is discussed by combining the results of this study with those of previous studies.

General geology

The Japanese Islands comprise a series of subduction-related rock units, including accretionary complexes, high-*P/T* metamorphic rocks, ophiolites, and arc igneous rocks that formed during the Phanerozoic (e.g., Wakita 2013; Kojima et al. 2016; Wakita et al. 2021). The proto-Japan is the archipelago formed before the Cretaceous, which was initiated by subduction during the Cambrian along the eastern margin of the Asian continent (e.g., Kimura and Hayasaka 2019; Sawada et al. 2022). It consists of the Paleozoic–Mesozoic accretionary complexes and high-*P/T* metamorphic belts and is mainly exposed in Southwest Japan and basically forms a piled nappe structure (e.g., Hayasaka 1987; Isozaki et al. 2010; Wakita et al. 2021). Those old complexes/belts are exposed on the continental side, with a younging trend toward the oceanic side

(Isozaki et al. 2010; Wakita 2013; Wakita et al. 2021). Paleozoic magmatic rocks rarely occur in the Japanese Islands (e.g., Fujii et al. 2008; Osanai et al. 2014; Kawaguchi et al. 2020; Kimura et al. 2019, 2021) without a batholith, except in the Hida Belt. The Hida Belt, which is characterized by late Paleozoic to Mesozoic gneisses, schists, and granitoids, is located along the most continental side of the Japanese Islands (Fig. 1), showing tectonic features that are different from the Phanerozoic accretionary complexes and high-*P/T* metamorphic belts in the Japanese Islands. The Hida Belt is thought to be a part of the continental margin and thrust over accretionary complexes and/or high-*P/T* metamorphic belts, leading to the present configuration (Komatsu et al. 1985; Sohma et al. 1990).

Hida Granites and Hida Metamorphic Belt

The Hida Belt is divided into three major subunits: the Permo–Triassic and Jurassic granitoids, including augen gneiss (Hida Granites), low-*P/T*-type gneisses and migmatites (Hida Metamorphic Belt), and medium-*P/T*-type schists (Unazuki Belt) (Fig. 2). Arakawa (1984) summarized the timing of multistage tectono-thermal events in the Hida Belt based on the Rb–Sr ages of gneisses and metamorphosed plutonic rocks; the late Silurian (first-stage) magmatism which represented by amphibolites, the middle Carboniferous (second-stage) magmatism which represented by mafic dykes, and the late Triassic to early Jurassic (third-stage) magmatism occurred in the continental margin or continental arc tectonic environments. Takahashi et al. (2018) suggested that the protoliths of the Hida metasedimentary rocks (paragneiss) were deposited during ~275–250 Ma, followed by metamorphism at ~250–235 Ma, with minor thermal events of ~270 Ma based on U–Pb dating of the zoned zircon grains. Cho et al. (2021) revealed that the intrusion of the orthogneiss occurred during the entire Permian period at ~302–254 Ma (Fig. 3), and was followed by solid-state recrystallization at ~250–240 Ma due to thermal overprinting from the intrusion of the Hida granitoids based on zircon U–Pb age dating. Suzuki et al. (1989) reported apparent metamorphic *P–T* conditions of ~730 °C and ~7 kbar from the high-grade parts of the Hida Metamorphic Belt. However, the timing of metamorphism and corresponding *P–T* conditions are not yet fully understood. The activity of the Hida granites can be divided into two major episodes, viz., ~260–230 Ma (Hida Older Granites) and ~200–180 Ma (Hida Younger Granites) (Sakoda et al. 2006; Horie et al. 2010, 2013, 2018; Takahashi et al. 2010, 2018; Zhao et al. 2013; Koizumi and Otoh 2019; Takehara and Horie 2019; Takeuchi et al. 2019, 2021; Cho et al. 2021; Yamada et al. 2021; Kawaguchi et al. 2023b) (Fig. 3b).

Unazuki Belt

The metamorphic rocks of the Unazuki area were suggested to be distinguishable from the metamorphic rocks in the other parts of the Hida Belt by the occurrence of staurolite and kyanite (Ishioka 1949). Hiroi (1978) divided the metamorphic rocks around the Unazuki area into the Unazuki Group, characterized by schist, and the Katakaigawa Group, characterized by gneiss. Hiroi et al. (1978) called the Unazuki Group the Unazuki schist. In this manuscript, we refer to the Unazuki schists and plutonic rocks intruding into the Unazuki area as the Unazuki Belt (Figs. 2 and 4). The Unazuki schist is composed of marble, pelitic schist, quartzo-feldspathic schists, and interlayers of pelitic and mafic schists in ascending order, probably conformably (Hiroi 1978; Fig. 4). The protoliths of quartzo-feldspathic

schists are considered felsic volcanic rocks and are traditionally called leptite (Ishioka and Suwa 1954, 1956). The Unazuki Belt and the Hida Metamorphic Belt are bounded by the Eboshiyama thrust fault (Hiroi 1978) (Fig. 4). In the eastern part of the Unazuki Belt, plutonic rocks intrude, and Unazuki schists disconnectedly occur as roof remnants (Hiroi 1978) (Fig. 4). Based on the symmetrical occurrences of the roof remnants and the well-zoned Unazuki schist layers in the western exposed area, Hiroi (1978) suggested the occurrence of a north−south-directed anticline named the Kurobe-Gawa anticline (Fig. 4). The pelitic schists of the Unazuki Belt contain chloritoid, staurolite, and kyanite, suggesting their medium-*P/T*-type metamorphism (Hiroi 1978, 1980), and their *P–T* conditions have been estimated to reach 650 °C and 6.7 kbar (Hiroi 1983). The age of the Unazuki schists is not well known, except for the late Carboniferous
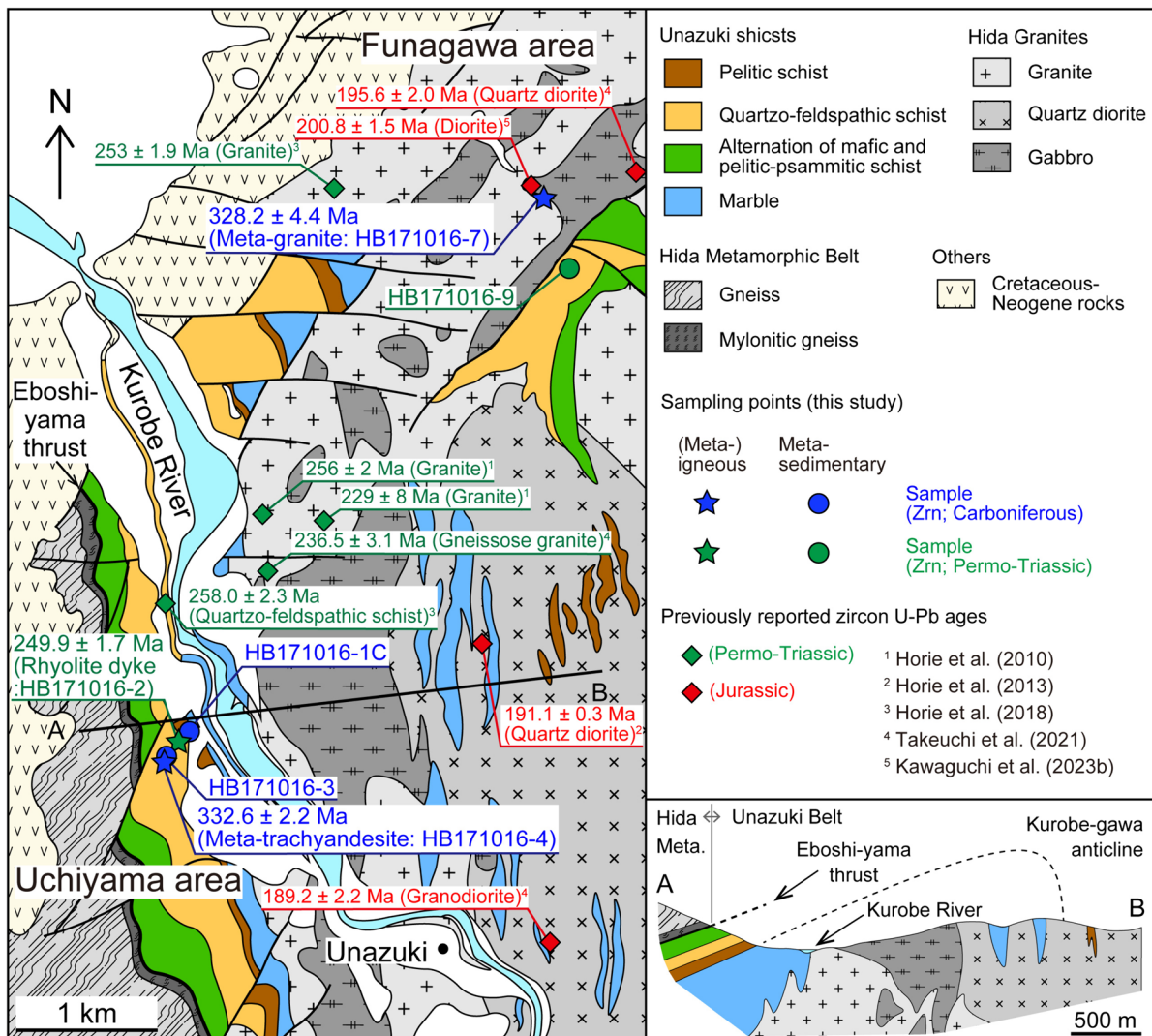

Fig. 4 Geological map of the northern part of the Unazuki Belt area, modified after Hiroi (1978) and Takeuchi et al. (2017). The mapped area is shown in Fig. 2

fossils in the siliceous part of the marble, which represents the timing of deposition for the lower structural unit of the Unazuki schists (Hiroi et al. 1978). In the Unazuki schists, biotite and muscovite Rb–Sr ages of 496 ± 35 Ma, 248 Ma, 240 ± 25 Ma, 234 ± 4 Ma, 227 ± 3 Ma, and 212 ± 2 Ma have been reported (Yamaguchi and Yanagi 1968, 1970; Shibata et al. 1970). Based on the occurrences of late Carboniferous fossils (Hiroi et al. 1978) and the above-mentioned Triassic Rb–Sr ages of the Unazuki Belt, Hiroi (1983) suggested that the protolith of the Unazuki schists was deposited between the Carboniferous and Permian ages that subsequently underwent medium-*P/T* metamorphism during the Permo–Triassic time. Recently, Horie et al. (2018) suggested that medium-*P/T* metamorphism occurred during ~ 258–253 Ma because 253.0 ± 1.9 Ma biotite granite contains a quartzo-feldspathic schist xenolith that probably has a magmatic age of 258.0 ± 2.3 Ma (Fig. 3).

The plutonic rocks in the Unazuki area are divided into metagabbro, quartz diorite, and granite (Fig. 4; Hiroi 1978), and they show two periods of magmatism at ~ 260–230 Ma and ~ 200–190 Ma with a gap of ~ 30 Myr (Horie et al. 2010, 2013, 2018; Takeuchi et al. 2021; Kawaguchi et al. 2023b; Fig. 3). Timing of magmatism of the igneous rocks in the Unazuki area shows a good correlation with that in the Hida Metamorphic Belt area (Fig. 3). The plutonic rocks in the Unazuki area are reported to have intruded into the Unazuki metamorphic rocks (Fig. 4; Hiroi 1978).

Petrography, field occurrences, and sample description

Two areas of the Unazuki Belt are the focus of this study; the Uchiyama area located in the south and the Funagawa area located in the north (Fig. 4).

Uchiyama area: The Grt–Hbl schist (HB171016-1C) has cm-size garnet with elongated hornblende and contains quartz, plagioclase, and chlorite as major phases (Fig. 5a). The rock shows clear schistosity represented by elongated hornblende (Fig. 5a). In the field, rhyolite (HB171016-2) occurs as a dyke cross-cutting the Unazuki schists. The rhyolite shows clear parallel joints which are different from the schistosity defined by the selective orientation of the metamorphic minerals which are typical for the Unazuki schists. This sample shows porphyritic plagioclase with fine-grained quartz and hornblende without clear foliation (Fig. 5b). Hbl–Bt schist (HB171016-3) shows clear schistosity (Fig. 5c). This rock is composed of quartz, plagioclase, biotite, and hornblende as major minerals (Fig. 5d). Metatrachyandesite (HB171016-4) has porphyroclastic plagioclase with biotite and quartz (Fig. 5e). Biotite in it imparts the schistosity (Fig. 5e). Due to the existence of porphyroclastic plagioclase with abundant quartz, this rock (HB171016-4) can be considered originally as a volcanic rock.

Funagawa area: Metagranite (HB171016-7) occurs as sporadic and minor outcrops of ~ 50 m in length along a narrow path and is bounded by a gray-colored gabbro–diorite pluton by the brittle fault with cataclasite and fault gouge. Metagranite is characterized by a pinkish surface due to abundant K-feldspar (Fig. 5f). Gabbrodiorite occurring close to the studied metagranite was dated to 200.8 ± 1.5 Ma by the zircon U–Pb method (Kawaguchi et al. 2023b; Fig. 4). The studied metagranite (HB171016-7) shows an equigranular texture and consists of quartz (~ 40 vol%), plagioclase (~ 30 vol%), K-feldspar (~ 25 vol%), and biotite (~ 5 vol%) as major phases (Fig. 5g). Biotite is partly replaced by chlorite (Fig. 5g). These microtexture and mineral assemblages represent a granitic origin. Hbl–Bt schist (HB171016-9) is a major rock facies in this area and shows clear schistosity in the field defined by the selective orientation of biotite and hornblende along with the interlayer of pelitic and psammitic layers, representing their sedimentary rock origin with interlayers of pelitic and psammitic parts (Fig. 5h, i).

Analytical methods

LA–ICP–MS zircon U–Pb age dating

Zircon U−Pb age dating of grains from the five Unazuki Belt samples (HB171016-1C, HB171016-3, HB171016-4, HB171016-7, and HB171016-9) was performed by a Nu Plasma II multicollector inductively coupled plasma mass spectrometer equipped with a New Wave Research 193-nm ArF excimer laser ablation system (LA–MC–ICP–MS) installed at the KBSI, Republic of Korea. To observe the internal texture of zircon, cathodoluminescence (CL) and backscattered electron (BSE) images were obtained using a scanning electron microscope (JEOL 6610LV) housed at the KBSI. Zircon 91500 (Wiedenbeck et al. 1995) was used as a primary standard to calibrate the U–Pb ratio. Plešovice zircon (Sláma et al. 2008) was selected as a consistency standard to confirm the data quality. A laser spot diameter of 15 μm and a laser repetition rate of 5 Hz were selected during the analysis. Each analysis consisted of approximately 20–30 s of background acquisition followed by 50 s of data acquisition. The weighted average ^{206}Pb/^{238}U age of the consistency standard, namely, the Plešovice zircon, was 338.6 ± 1.4 Ma (MSWD = 0.55, $n = 23$), which is consistent with the recommended value (337.13 ± 0.37 Ma; Sláma et al. 2008).

Zircon U–Pb age dating and trace element analysis of zircon grains from the rhyolite dyke in the Unazuki Belt (HB171016-2) were simultaneously performed by a GeolasPro laser ablation system that consists of a COMPexPro 102 ArF excimer laser coupled with an Agilent 7900e ICP–MS instrument housed at the Wuhan Sample Solution
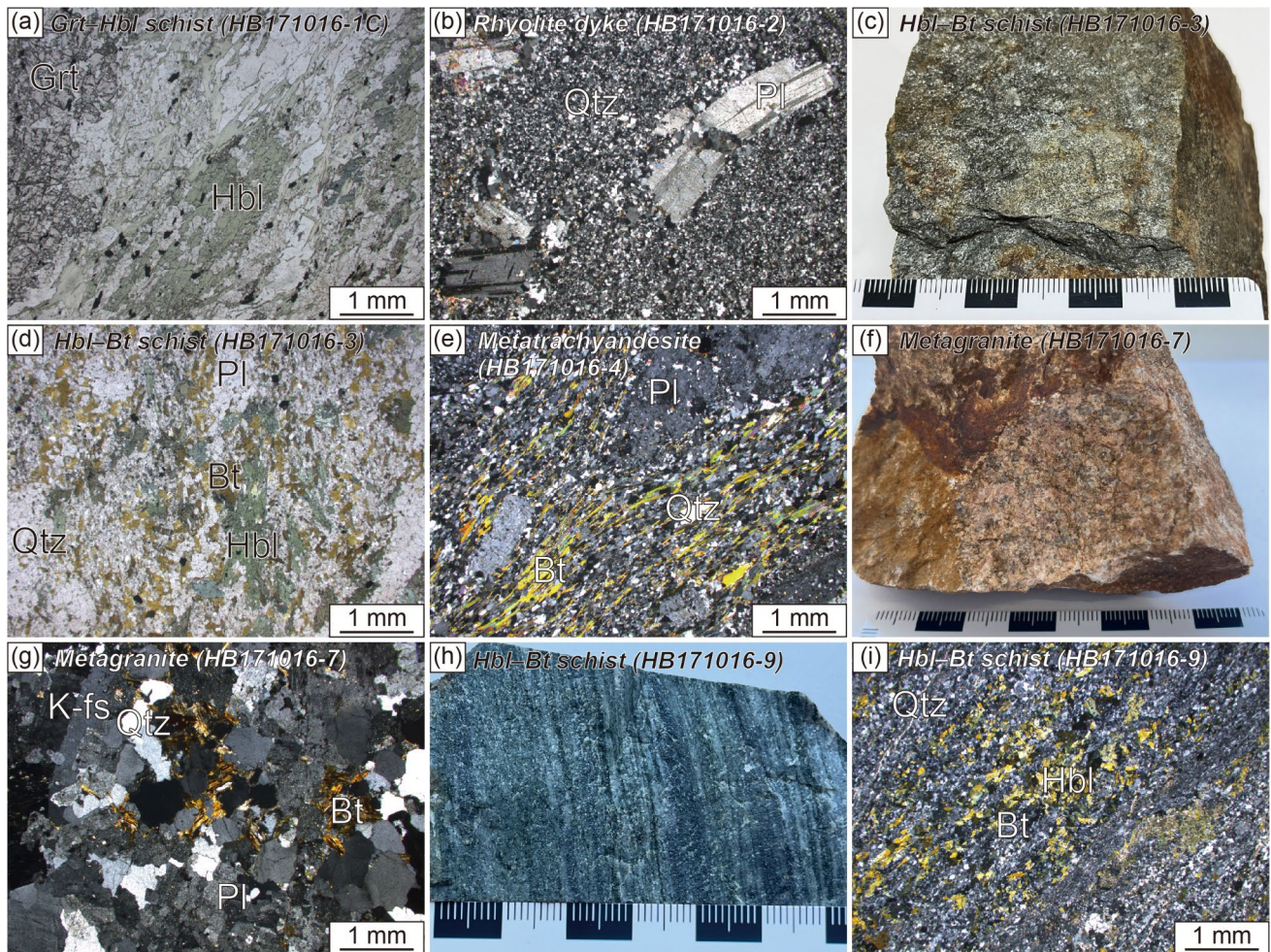
Fig. 5 Sample photographs and photomicrographs of the studied rocks of the Unazuki Belt. **a** Photomicrograph of the Grt–Hbl schist (HB171016-1C). **b** Photomicrograph of the rhyolite dyke (HB171016-2). **c**, **d** Sample image and photomicrograph of the Hbl–Bt schist (HB171016-3). **e** Photomicrographs of the metatra-chyandesite (HB171016-4). **f**, **g** Sample photograph and photomicrograph of the metagranite (HB171016-7). **h**, **i** Sample image and photomicrograph of the Hbl–Bt schist (HB171016-9). *Bt* biotite, *Hbl* hornblende, *Kfs* K-feldspar, *Grt* garnet, *Pl* plagioclase, *Qtz* quartz

Analytical Technology Co., Ltd, Hubei, China. Helium gas was used as a carrier gas to transport the abraded sample. Argon gas was mixed with the carrier gas before entering the ICP–MS. Zircon 91500 (Wiedenbeck et al. 1995) and glass standard NIST610 (Stephen and Robert 2012) were used as primary standards to calibrate the U–Pb ratio and trace element concentration, respectively. Plešovice zircon (Sláma et al. 2008) was selected as a consistency standard to confirm the data quality. A laser spot diameter of 32 μm and a laser frequency of 5 Hz were selected during the analysis. Each analysis consisted of approximately 20–30 s of background acquisition followed by 50 s of data acquisition. Trace element compositional analysis of zircon was further calibrated with Si as an internal standard. Data reduction was conducted by ICPMSDataCal software (Liu et al. 2008, 2010). Concordia plotting and weighted average age calculations were conducted by Isoplot/EX_ver3 (Ludwig 2003). Detailed analytical and calculation processes are described in Zong et al. (2017) and Kawaguchi et al. (2023a). The concordia age and weighted average $^{206}Pb/^{238}U$ age of the consistency standard, namely, the Plešovice zircon, were 337.8 ± 1.3 Ma (MSWD = 0.11, $n = 7$), and 337.8 ± 2.5 Ma (MSWD = 0.41, $n = 7$), respectively, which are consistent with the recommended value (337.13 ± 0.37 Ma; Sláma et al. 2008).

Throughout this study, concordant data are defined as a discordance level (difference between $^{206}Pb/^{238}U$ and $^{207}Pb/^{235}U$ dates) of less than 10%. In this study, $^{206}Pb/^{238}U$ dates are used for zircon grains younger than 1000 Ma, whereas $^{207}Pb/^{206}Pb$ dates are used for zircon grains older than 1000 Ma. The weighted mean age is quoted at the 95% confidence level, and the dates and isotopic ratios are at the

2σ confidence level. All the LA–ICP–MS zircon U–Pb age dating results are listed in Supplementary Table S1.

Zircon Lu–Hf isotope analysis

Lu–Hf isotope analysis of zircon grains from the five Unazuki Belt samples (HB171016-1C, HB171016-3, HB171016-4, HB171016-7, and HB171016-9) was performed using LA–MC–ICP–MS at the KBSI. Analytical spots were chosen at the same zoned points of the U–Pb dating under a laser diameter of 44 μm. The energy density of laser ablation was maintained at ~7.0 J/cm^2. Each analysis consisted of 20 s of background acquisition followed by 50 s of ablation signal acquisition. Zircon 91500 was used as a primary standard to calibrate the isotopes, and zircon FC1 was used as a consistency standard to confirm the data quality. During the analysis, the ^{176}Hf/^{177}Hf ratio of zircon FC1 was 0.282168 ± 0.000014 (95% confidence interval; $n = 19$), which is consistent with the reference values (Woodhead and Hergt 2005).

Zircon Lu–Hf isotope analysis of the rhyolite dyke in the Unazuki Belt (HB171016-2) was conducted using a Neptune Plus MC–ICP–MS coupled with a GeoLas HD excimer ArF laser ablation system (Coherent, Götingen, Germany) housed at the Wuhan Sample Solution Analytical Technology Co., Ltd., Hubei, China. Helium gas was used as a carrier gas and merged with argon gas after the ablation cell. A small volume of nitrogen gas was used to improve the sensitivity. Analytical spots were selected at the same zoned points of the U–Pb dating under a laser diameter of 44 μm. The energy density of laser ablation was maintained at ~7.0 J/cm^2. Each analysis consisted of 20 s of background acquisition followed by 50 s of ablation signal acquisition. Detailed analytical conditions are the same as those described by Hu et al. (2012). Plešovice zircon was used as a primary standard to calibrate the isotopes, and zircon grains from samples 91500 and GJ-1 were used as secondary standards to monitor the data quality. During the analysis, the ^{176}Hf/^{177}Hf ratios of zircon grains from samples 91500 and GJ-1 are 0.282313 ± 0.000014 (95% confidence interval; $n = 4$) and 0.282020 ± 0.000014 (95% confidence interval; $n = 4$), respectively, which are consistent with the reference values (Goolaerts et al. 2004).

Throughout this study, the ^{176}Lu decay constant of 1.867×10^{-11} year^{-1} (Söderlund et al. 2004) was selected to obtain the initial ^{176}Hf/^{177}Hf ratio. The $\varepsilon_{Hf}(t)$ values were calculated using the reference chondritic values of ^{176}Hf/^{177}Hf $= 0.282772$ and ^{176}Lu/^{177}Hf $= 0.0332$ (Blichert-Toft and Albarède 1997). The single-stage Hf model age (T$_{DM1}$) was calculated using ^{176}Lu/^{177}Hf and ^{176}Lu/^{177}Hf values of 0.28325 and 0.0384, respectively, which represent the depleted mantle (Griffin et al. 2002), and the two-stage Hf model age (T$_{DM2}$) was calculated using the ^{176}Lu/^{177}Hf

value of 0.015, which represents an average continental crust (Griffin et al. 2002). All the LA–MC–ICP–MS zircon Lu–Hf isotope results are listed in Supplementary Table S2.

Whole-rock geochemical analysis

Whole-rock chemical analysis was conducted at Activation Laboratories Ltd., Ancaster, Ontario, Canada. Before the analysis, fresh samples without any veins and weathered portions were crushed into a fine powder. The major and trace element concentrations were determined using inductively coupled plasma atomic emission spectrometry (ICP–AES; Termo Jarrel-Ash ENVIRO II) and inductively coupled plasma−mass spectrometry (ICP–MS; Perkin Elmer Optima 3000). The detailed sample preparation and analysis procedures are described in Lee et al. (2016). All the whole-rock chemical data are listed in Supplementary Table S3, together with the GPS sampling points.

Results

LA–ICP–MS zircon U–Pb ages

Carboniferous metaigneous rock: Zircon grains separated from the metatrachyandesite (HB171016-4) are colorless and reach 250 μm along the longer axis. They show euhedral shapes and aspect ratios of mostly 1:1 to 1:2. All the separated zircon grains show oscillatory zoning without clear rims, as evidenced by the CL images (Fig. 6a). One hundred twenty spots were chosen, and one hundred fourteen spots yielded concordant dates (Fig. 7a). All the analyzed spots show Carboniferous dates without older inherited ages (Fig. 7a). The weighted mean ^{206}Pb/^{238}U age is 332.6 ± 2.2 (MSWD $= 0.34$, $n = 114$) (Fig. 7a). The Th/U ratios of concordant data are 0.16–1.05.

Zircon grains separated from metagranite (HB171016-7) also have colorless and euhedral grains, their sizes reach 250 μm along the longer axis, and they have length:width ratios of approximately 1:1.5–1:3. All the separated zircon grains show clear oscillatory zoning without rims, and a few of the grains have cores, as evident in the CL image (Fig. 6b). Forty-five spots, including zircon cores, have been analyzed, and forty-one spots show concordant dates (Fig. 7b). All concordant dates, including those from cores, show a Carboniferous single age cluster without any older inherited age (Fig. 7b). The weighted mean ^{206}Pb/^{238}U age is 328.2 ± 4.4 (MSWD $= 0.28$, $n = 41$) (Fig. 7b). The Th/U ratios of concordant data are 0.16–0.54.

Permo–Triassic rhyolite dyke: Zircon grains extracted from the rhyolite dyke (HB171016-2) are euhedral to subhedral in shape and colorless. Their sizes are up to 150 μm along the longer axis, with aspect ratios of 1:1 to 2:1. They

Fig. 6 CL images of the studied zircon grains from the Unazuki Belt. The U−Pb dating spots and Lu−Hf analytical spots are shown by solid and dashed circles, respectively. The dates with 2σ error and ε_Hf(t) values are shown for each spot
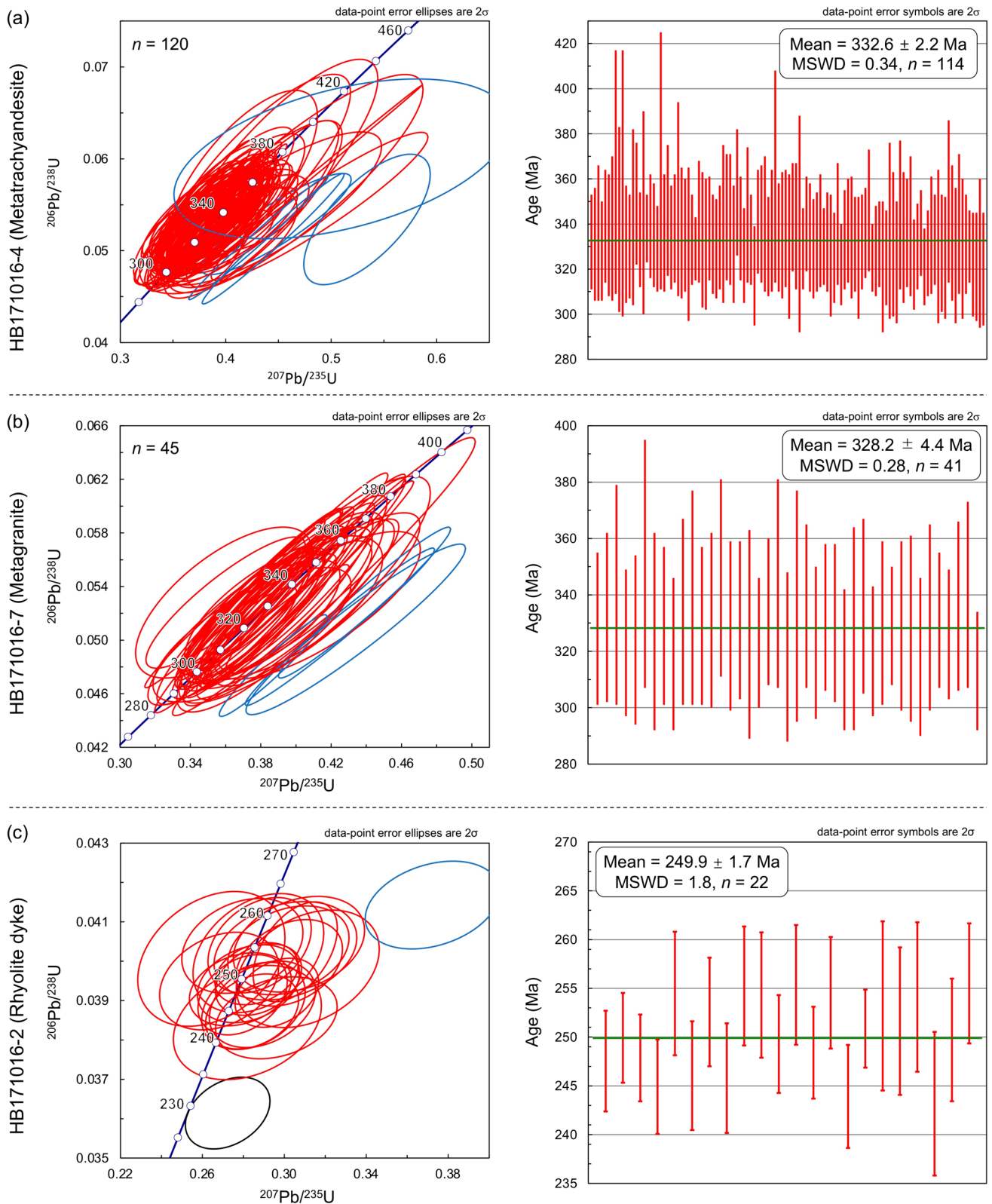
Fig. 7 Concordia plots and weighted mean age diagrams of the (meta-)igneous rocks from the Unazuki Belt. **a** Metatrachyandesite (HB171016-4). **b** Metagranite (HB171016-7). **c** Rhyolite dyke (HB171016-2)

show clear oscillatory zoning in the CL image (Fig. 6c). Twenty-four analyses for twenty-four grains were conducted, and twenty-three spots yielded concordant dates (Fig. 7c). Concordant dates show a weighted mean $^{206}Pb/^{238}U$ age of 249.9 ± 1.7 Ma (MSWD = 1.8, $n = 22$), with one rejected younger date (Fig. 7c). The Th/U ratios of the concordant dates range from 0.34–1.09.

Carboniferous metasedimentary rocks: Zircon grains obtained from Grt–Hbl schist (HB171016-1C) are colorless, and their sizes are up to 200 μm along the longer axis. They show euhedral to subhedral shapes and aspect ratios of 1:1.5 to 1:3. Oscillatory zoning is commonly observed in the zircon in the CL images (Fig. 6d). Twenty-three points have been analyzed, and twenty-one spots yield concordant dates ranging from ~ 320 to ~ 300 Ma with a

single peak age at ~ 310 Ma and without any older grains (Fig. 8a). The youngest detrital zircon is 298 Ma (Fig. 8a). The Th/U ratios of the zircon grains with concordant dates show values between 0.33 and 1.12.

Zircon grains extracted from Hbl–Bt schist (HB171016-3) are colorless and reach 180 μm along the longer axis. They show euhedral to subhedral shapes and aspect ratios of mostly 1:1 to 1:1.5. Separated zircon grains commonly show oscillatory zoning in CL images (Fig. 6e). Forty-two points have been analyzed, and forty points show concordant dates ranging from ~ 360 Ma to ~ 305 Ma (Fig. 8b), with Th/U ratios of 0.36 to 1.28. The youngest detrital zircon yields an age of 305 Ma, and all the concordant dates mark a single peak age at ~ 320 Ma (Fig. 8b).
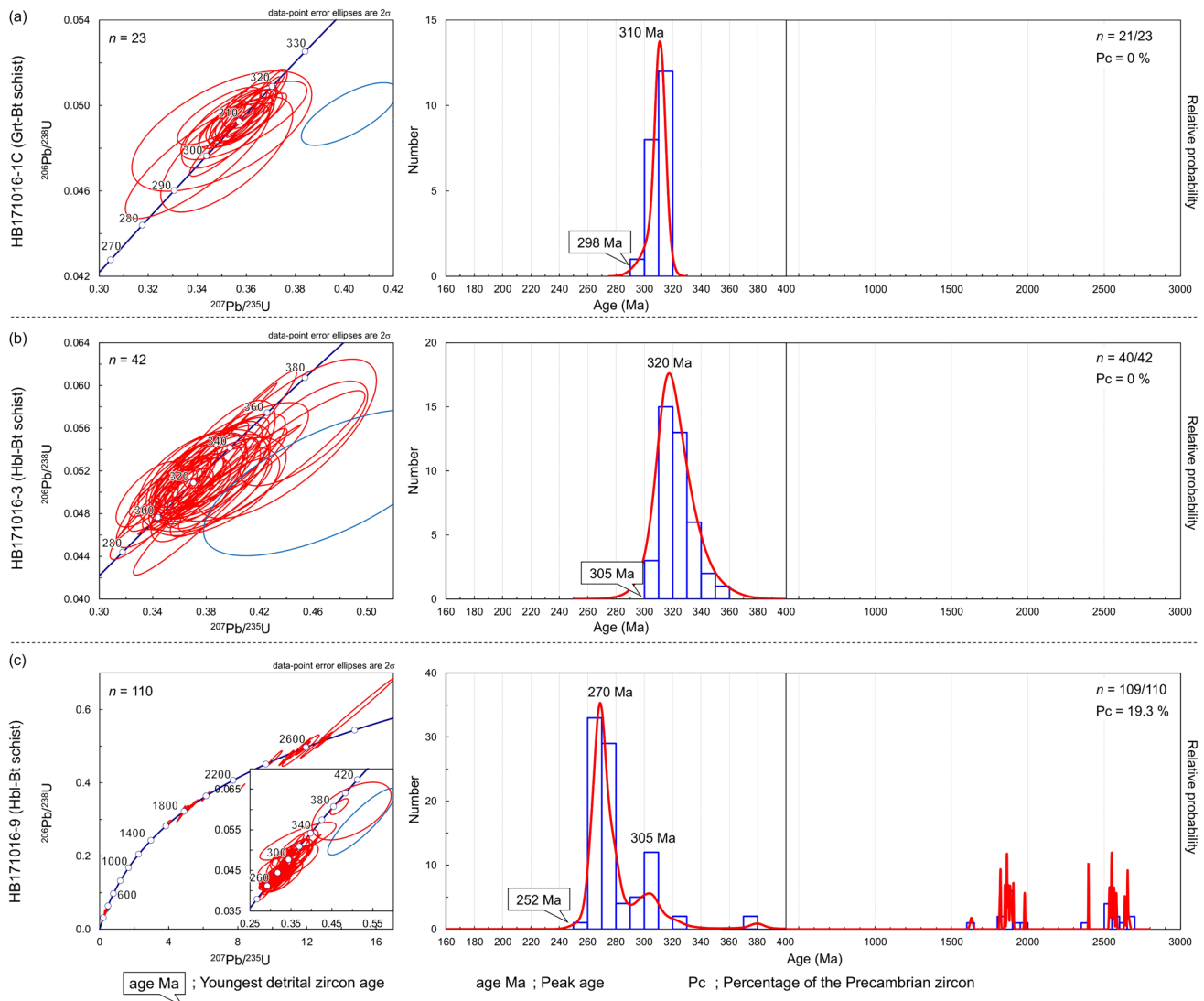

Fig. 8 Concordia plots and age histograms with probability density diagrams of the metasedimentary rocks from the Unazuki Belt. **a** Grt–Hbl schist (HB171016-1C). **b** Hbl–Bt schist (HB171016-3). **c** Hbl–Bt schist (HB171016-9)

Permo–Triassic metasedimentary rock: Zircon grains obtained from Hbl–Bt schist (HB171016-9) are euhedral to subhedral in shape, and their sizes are up to 200 μm along the longer axis, with aspect ratios of 1:1 to 2:1. Most of the separated zircon grains show oscillatory zoning, as evidenced from the CL images (Fig. 6f). One hundred ten points have been analyzed, and one hundred nine points show concordant dates from the Archean to late Permian (Fig. 8c). The youngest detrital zircon shows an age of ~ 252 Ma, and the most prominent peak is at ~ 270 Ma, with 19.3% of Precambrian detrital grains (Fig. 8c). The Th/U ratios of the concordant dates are 0.17–2.75.

LA–MC–ICP–MS zircon Lu–Hf isotopes

The $\varepsilon_{Hf}(t)$ values of zircon grains from Carboniferous metaigneous rocks are between + 4.38 and + 16.72 for HB171016-4 and + 13.50 and + 18.00 for HB171016-7, and those of the Carboniferous metasedimentary rocks are between + 6.21 and + 15.75 for HB171016-1C and between + 11.46 and + 14.87 for HB171016-3 (Fig. 9). The Early Triassic rhyolite dyke (HB171016-2) yields $\varepsilon_{Hf}(t)$ values of + 10.77 to + 12.51 (Fig. 9). The $\varepsilon_{Hf}(t)$ values of the late Permian Hbl–Bt schist (HB171016-9) show wide variations ranging from + 13.25 to -25.50 (Fig. 9).

Whole-rock geochemistry

The metagranite (HB171016-7) shows SiO_2 and total alkali contents of 77.2 wt% and 7.55 wt%, respectively, showing a granitic composition (Fig. 10a). It is characterized as a high-K series (Fig. 10c). The (meta-)igneous rocks of HB171016-2 and HB171016-4 show SiO_2 contents of 74.9 and 61.7 wt%, with total alkali contents of 8.89 and 7.41 wt%, respectively, showing rhyolite (HB171016-2) and

trachyandesite (HB171016-4) compositions (Fig. 10b). They are high-K series rocks (Fig. 10c). The metagranite (HB171016-7) and metatrachyandesite (HB-171016-4) show enrichments in light rare earth elements (LREEs) with depletions in heavy rare earth elements (HREEs) in a C1 chondrite-normalized REE diagram, without significant Eu anomalies (Fig. 11a). They show Nb–Ta troughs with negative Ti anomalies (Fig. 11b). Three (meta-)igneous rocks (HB171016-2, HB171016-4, and HB171016-7) are commonly plotted within volcanic arc granite tectonic setting fields in tectonic diagrams using trace elements (Fig. 12a–e) and show typical arc characters, without an adakitic nature (Fig. 12f).

The five metasedimentary rocks (HB171016-1, HB171016-1B, HB171016-1C, HB171016-3, and HB171016-9) show a wide range of SiO_2 contents of 55.4 to 63.7 wt% (Fig. 10b). Four samples (HB171016-1, HB171016-1B, HB171016-1C, and HB171016-3) show low total alkali contents of 1.33 to 3.12 wt% (Fig. 10b) with the extremely low K_2O contents of less than 1.25 wt% (Fig. 10c). In contrast, one sample (HB171016-9) has a relatively high total alkali content of 6.64 wt% (Fig. 10b), with medium K_2O contents of 2.12 wt% (Fig. 10c). They show enrichments in LREEs with depletions in HREEs, without significant negative Eu anomalies, similar to the (meta-)igneous rocks from the Unazuki Belt (Fig. 11a). They are commonly depleted in Nb, Ta, and Ti, similar to the (meta-)igneous rocks in the Unazuki Belt (Fig. 11b).
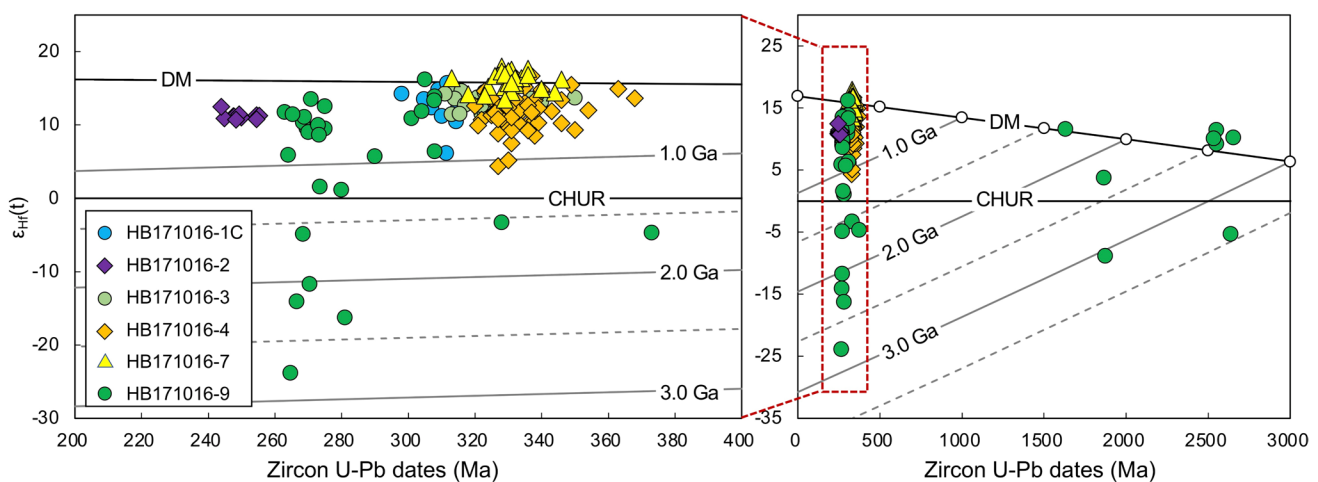

Fig. 9 Zircon U–Pb dates vs. $\varepsilon_{Hf}(t)$ values of zircon grains from the studied rocks from the Unazuki Belt
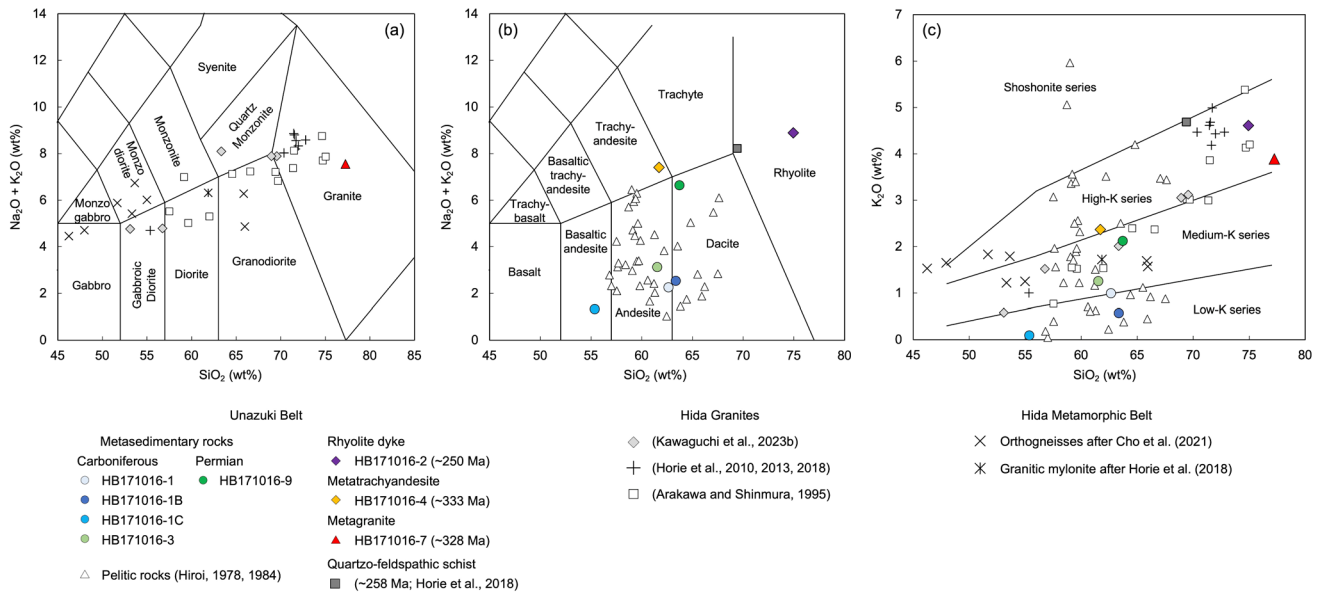
Fig. 10 Plot of whole-rock data from the Unazuki Belt, from this and previous studies. **a** Total alkali vs. silica (TAS) classification diagram for plutonic rocks after Middlemost (1994). **b** TAS classification diagram for the volcanic rocks after Middlemost (1994). **c** SiO$_2$ (wt%) vs. K$_2$O (wt%) classification diagram after Peccerillo and Taylor (1976)
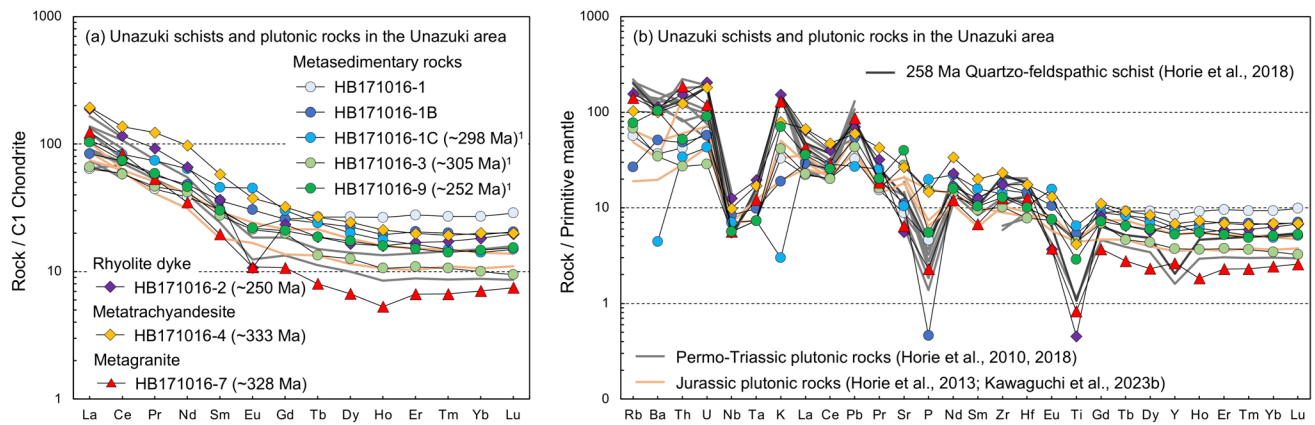

Fig. 11 C1 chondrite-normalized REE patterns (**a**) and primitive mantle-normalized multielement patterns (**b**) for the studied rocks from the Unazuki Belt and those of the previously reported data from the same Belt. Normalized values are after Sun and Mcdonough (1989)

Discussion

Carboniferous island arc magmatism in the Unazuki Belt

The comprehensive geochronology of the Unazuki Belt has not yet been clearly determined. In this study, important zircon U–Pb ages for determining the Carboniferous tectono-thermal events of the Unazuki Belt were obtained for the first time. The Carboniferous intermediate volcanism and felsic plutonism at 332.8 ± 2.2 Ma (HB171016-4; Fig. 7a) and 328.2 ± 4.4 Ma (HB171016-7; Fig. 7b),

respectively, were confirmed in the Unazuki Belt (Figs. 3 and 4). Zhao et al. (2013) proposed the possible ~330 Ma regional tectono-thermal event of the Hida Belt based on the single inherited zircon U–Pb date on the oscillatory-zoned core (329.9 ± 6.3 Ma) from the 243 ± 8 felsic gneiss; however, the tectonic interpretation at ~330 Ma was unclear. In addition, although a whole-rock Rb–Sr isochron age of 332 ± 74 Ma was reported from the meta-tonalite in the Hida Belt (Arakawa 1984), the accurate timing of magmatism is uncertain due to its large error value. Therefore, certain ~330 Ma magmatic rocks have not been reported thus far from the Hida Belt, including the Unazuki Belt, and the suspected ~330 Ma tectono-thermal
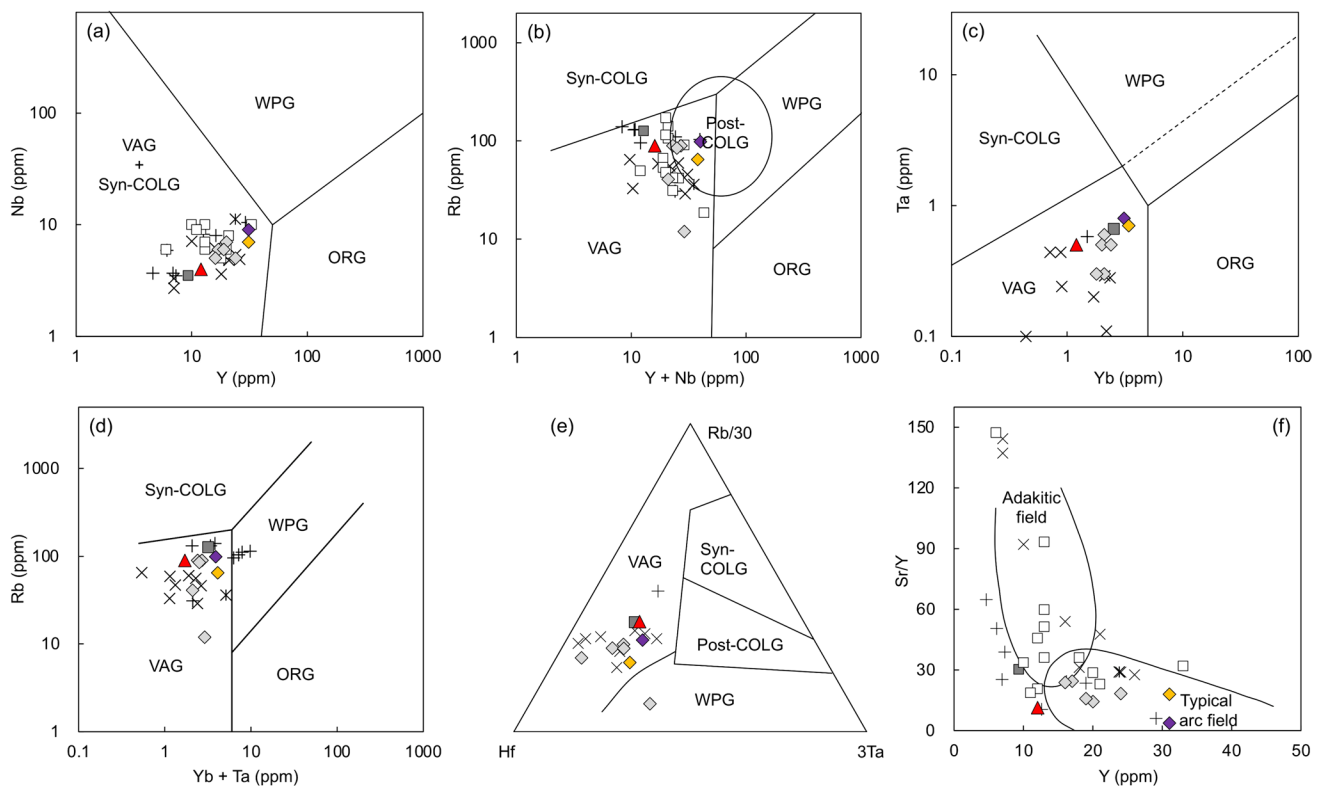
Fig. 12 Whole-rock trace element compositions for granitic rocks plotted on various tectonic discrimination diagrams, including Nb vs. Y (**a**), Rb vs. Y+Nb (**b**), Ta vs. Yb (**c**), and Rb vs. Yb+Ta (**d**) diagrams after Pearce et al. (1984), Rb/30-Hf-3*Ta diagram (**e**) after Harris et al. (1986), and the Y (ppm) vs. Sr/Y diagram (**f**) after Defant et al. (1991). VAG: volcanic arc granite; ORG: ocean ridge granite; WPG: within-plate granite; Syn-COLG: syn-collisional granite; Post-COLG: post-collisional granite. The legends are the same as those shown in Fig. 10. The data sources of the previous studies are the same as those used in Fig. 10

event has been highly uncertain for a long time. No significant Ce anomaly in the whole-rock composition is one of the indicators to evaluate the element mobility, and the whole-rock Ce/Ce* values of the studied metagranite and metatrachyandesite plot in the range between 0.89 and 1.03 (Fig. 11a, Supplementary Table S3), suggesting that the rocks have not been significantly affected by later elemental modification during the metamorphism (Polat et al. 2002). The whole-rock compositions of ~ 330 Ma metagranite and metatrachyandesite show enrichments in LREEs compared to those of HREEs without significant Eu anomaly (Fig. 11a) and clear Nb–Ta troughs along with Ti and P depletions (Fig. 11b), suggesting a subduction-related arc signature. Moreover, tectonic discrimination diagrams using trace elements clearly show that Carboniferous felsic and intermediate magmatism occurred in a volcanic arc tectonic setting (Fig. 12a–e). The $\varepsilon_{Hf}(t)$ values of zircon grains from the 332.8 ± 2.2 Ma metatrachyandesite (HB171016-4; Fig. 7a) and those from 328.2 ± 4.4 Ma metagranite (HB171016-7; Fig. 7b) are close to the depleted mantle (DM) line (Fig. 9), suggesting that the source materials are not the East Asian continental

craton but the depleted mantle materials and/or their crustal derivatives with very minor contamination by old crustal material. These data indicate that they were generated in the tectonic setting such as an island arc located away from the continental craton.

Provenance and tectonic setting of the metasedimentary rocks in the Unazuki Belt

The youngest detrital zircon grains in the two metasedimentary rocks from the Unazuki Belt give ages of ~ 298 Ma and ~ 305 Ma, and they have only a single cluster at ~ 320–300 Ma and ~ 360–305 Ma, respectively, without any Pre-360 Ma detrital zircon (Fig. 8a, b). As Precambrian rocks are some of the main basements along the margin of the East Asian continent (e.g., Lee et al. 2016; Wang et al. 2020a, b; Kang et al. 2023), Precambrian detrital zircon should be found in sedimentary rocks deposited along the East Asian continent. Therefore, the absence of Precambrian detrital zircon as well as their Carboniferous single clusters (Fig. 8a, b) indicates that the source crust was solely

Carboniferous crust that separated from the East Asian continental craton.

The studied metasedimentary rocks can be considered to have experienced a certain degree of metamorphism due to the occurrences of the metamorphic minerals including garnet and hornblende. However, the whole-rock Ce/Ce* values of the studied metasedimentary rocks plot in the range between 0.88 and 1.11, suggesting that the rocks had not been significantly affected by elemental modification during the metamorphism (Polat et al. 2002). Carboniferous metasedimentary rocks of the Unazuki Belt have high Al_2O_3 and low K_2O contents of 12.08–18.58 wt% and 0.09–1.25 wt%, respectively (Supplementary Table S3), and the previously reported whole-rock geochemical data of the metasedimentary rocks of the Unazuki Belt show similar Al_2O_3 values of 16.80–21.87 wt% and K_2O values of 0.39–1.51 wt% (Hiroi 1978). Although the timing of deposition for the previously reported samples is unclear, they were mostly collected from the same lithological horizon in which our Carboniferous metasedimentary rocks were collected (HB171016-1C and HB171016-3) along the Kurobe River area (Fig. 4) and sharing a similar geochemical affinity as mentioned above, indicating that the majority of them likely have Carboniferous depositional ages. Their whole-rock geochemical characteristics including the high Al_2O_3 and low K_2O contents are considered to be quite different from those of trench-fill sediments, including the accretionary complex and its metamorphosed equivalent (Ehiro et al. 2016). Moreover, the lithological assemblage of the Unazuki schists is characterized by the occurrences of bimodal volcanic rocks, high-aluminous metapelite, and impure marbles without chert (Hiroi 1978; Fig. 4), suggesting their different lithological characteristics from the trench-fill sediments. Instead, considering those chemical characteristics along with the lithological assemblage, metasedimentary rocks of the Unazuki schists were suggested to have been deposited in a rifted continental margin (Sohma et al. 1990; Sohma and Kunugiza 1993). In the tectonic discrimination diagrams using major and trace elements, the Carboniferous metasedimentary rocks of the Unazuki Belt along with the previously reported pelitic schists of the Unazuki Belt (Hiroi 1978, 1984) show a good correlation with the geochemical characteristics of the oceanic island arc sediments (Figs. 13 and 14). Moreover, the island arc source provenance for the metasedimentary rocks of the Unazuki Belt is clearly supported by the Lu–Hf isotopes of detrital zircon grains. The Carboniferous detrital zircon grains from the metasedimentary rocks (HB171016-1C and HB171016-3) commonly have positive $\varepsilon_{Hf}(t)$ values close to the DM line (Fig. 9), suggesting that the detrital zircon grains in the studied Carboniferous metasedimentary rocks were sourced from the Carboniferous crusts originated from the depleted mantle and/or its crustal derivatives without significant input of old crustal materials, indicating that they
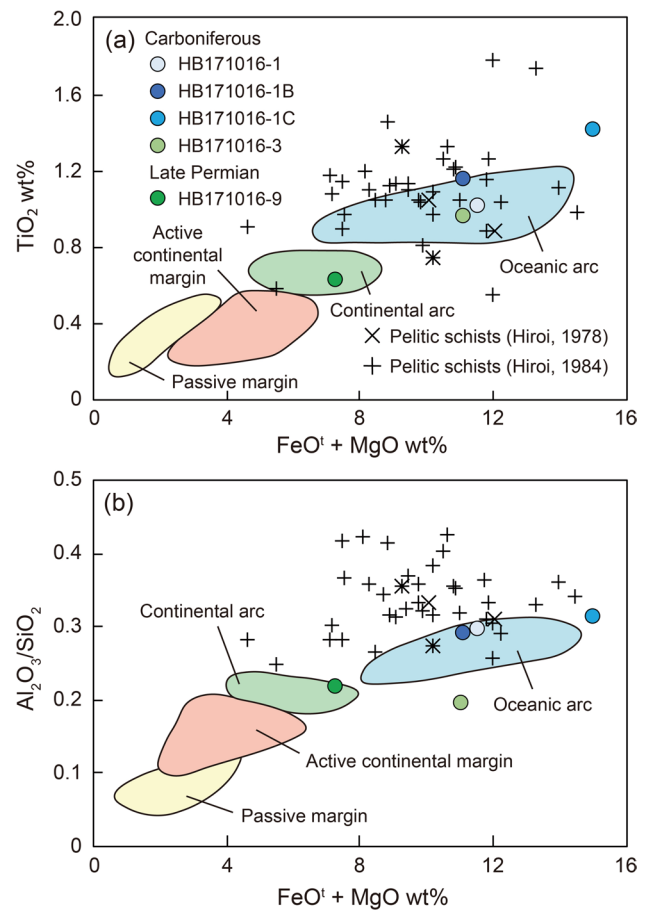

Fig. 13 Plots of whole-rock compositions of the Carboniferous and Permian metasedimentary rocks in the Unazuki Belt from this and previous studies on tectonic discrimination diagrams for sedimentary rocks using major element data after Bhatia (1983)

were formed under an island arc tectonic setting. Magmatic zircon grains in the ~330 Ma metagranite (HB171016-7) and metatrachyandesite (HB171016-4) in the Unazuki Belt show positive $\varepsilon_{Hf}(t)$ values that are similar to the Carboniferous detrital zircon grains (Fig. 9), implying that they are one of the source materials for the Carboniferous metasedimentary rocks of the Unazuki Belt. The rocks with island arc geochemical affinities are reported to have been generated not only from the ocean-ocean subduction-related island arc but also from the island arc formed within the thin and juvenile continental crust (~30–35 km), such as a continental margin (e.g., Harmon and Barreiro 1984; Winter 2014). All evidence, including the lithological assemblage, geochemical data, zircon U–Pb ages, and Lu–Hf isotopes of zircon, supports that the protolith of the metasedimentary rocks of the Unazuki Belt deposited next to the isolated Carboniferous island arc originally generated within a thin and juvenile continental margin.

However, the presence of Precambrian detrital zircon grains (~20%) in the Hbl–Bt schist (HB171016-9), with
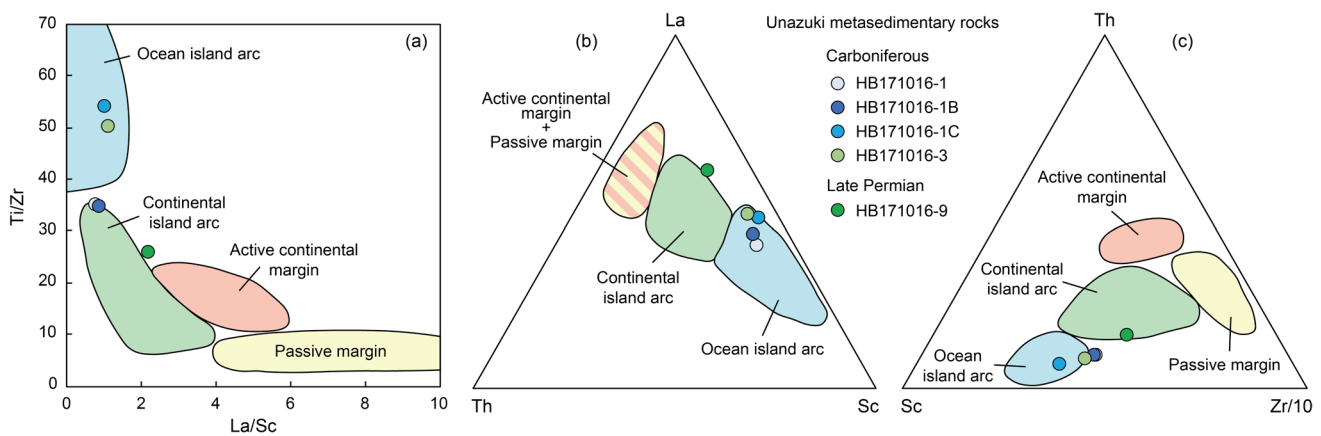
Fig. 14 Plots of whole-rock compositions of the Carboniferous and Permian metasedimentary rocks in the Unazuki Belt from this study on the tectonic discrimination diagrams for the sedimentary rocks using trace element data after Bhatia and Crook (1986)

the youngest detrital age of ~ 252 Ma (Fig. 8c), indicates that at ~ 252 Ma, the sedimentary rocks of the Unazuki Belt were deposited in the continental arc to which Precambrian detrital zircon grains were supplied from the continental craton. Moreover, the ~ 280–260 Ma detrital zircon grains in the Hbl–Bt schist (HB171016-9) yielded wide variations in $\varepsilon_{Hf}(t)$ values from + 16.3 to -25.5 (Fig. 9) and corresponding T_{DM2} ages of ~ 3000–280 Ma, indicating a continental arc tectonic setting at ~ 252 Ma in which zircon grains were formed from both juvenile and mature crustal sources. Considering the age dating results in this study, along with the previously suggested depositional age of the limestone (Hiroi et al. 1978) and the lithological sequence of the Unazuki schists (Hiroi 1978), the evolutional history of the Unazuki Belt can be constrained as follows: (1) lowermost limestone formed during the Carboniferous and (2) subsequent felsic and intermediate island arc igneous activities occurred at least at ~ 333–328 Ma, (3) followed by the deposition of the clastic rocks at least at ~ 300 Ma, which solely have a Carboniferous island arc crust origin. These results suggest that in the Unazuki Belt, there was a transition from island arc to continental arc environments between ~ 300 Ma and ~ 250 Ma, indicating that the collision between the island arc and continental margin might have occurred sometime between ~ 300 Ma and ~ 250 Ma and that the intermediate-*P/T* metamorphism can be related to this collision process. Considering that foliation is well-developed in the Hbl–Bt schist with the youngest detrital zircon age of ~ 252 Ma (Figs. 5h, i, and 8c) but not in the rhyolite dyke with an intrusion age of 249.9 ± 1.7 Ma (Figs. 5b and 7c), the collision process that caused the intermediate-*P/T* metamorphism might have continued until ~ 252 Ma but possibly terminated before ~ 250 Ma. In a previous study, intermediate-*P/T* metamorphism was considered to have occurred during ~ 258–253 Ma (Horie et al. 2018) in the Unazuki Belt. Therefore, 252–250 Ma could be the timing

of termination for the intermediate-*P/T* metamorphism of the Unazuki Belt related to the collision between the island arc and continental margin. In the Unazuki Belt, the emplacement ages of the magmatic rocks show two periods of ~ 255–230 Ma and ~ 200–190 Ma (Fig. 3), and they show arc signatures in their whole-rock compositions (Horie et al. 2010; Kawaguchi et al. 2023b; this study) (Figs. 11, 12, 13, 14), suggesting that subduction occurred at least during ~ 255–230 Ma and ~ 200–190 Ma in the Unazuki Belt.

Tectonic evolution of the Unazuki Belt from the Carboniferous to Triassic

During the Early Carboniferous, subduction occurred along the East Asian continental margin causing high-*P/T*-type metamorphism, including eclogite-facies metamorphism reported from the Hida Gaien Belt (Yoshida et al. 2020). The Early Carboniferous high-*P/T*-type metasedimentary rocks in the Hida Gaien Belt include significant amounts of Precambrian and Early Paleozoic detrital zircon grains (Yoshida et al. 2020), suggesting that the subduction zone was located along the East Asian continental margin (Fig. 15a). Before ~ 330 Ma, rifting might have occurred within the thin and juvenile continental margin, leading to the formation of an island arc that was separated from the continental margin (Fig. 15b), as evident from the occurrences of bimodal volcanism and the geochemical characteristics of the metasedimentary rocks of the Unazuki Belt, including their high Al_2O_3 contents and high Fe^{3+}/Fe^{2+} ratios. During this time, island arc igneous activity occurred, as evident from the ages of island arc magmatism (332.6 ± 2.2 Ma and 328.2 ± 4.4 Ma; Fig. 7a, b) and those of the detrital zircon grains from the Carboniferous metasedimentary rocks in the Unazuki Belt (~ 360–300 Ma; Fig. 8a, b) (Fig. 15b). High positive $\varepsilon_{Hf}(t)$ values of the Carboniferous zircon grains (Fig. 9) also suggest that the island arc
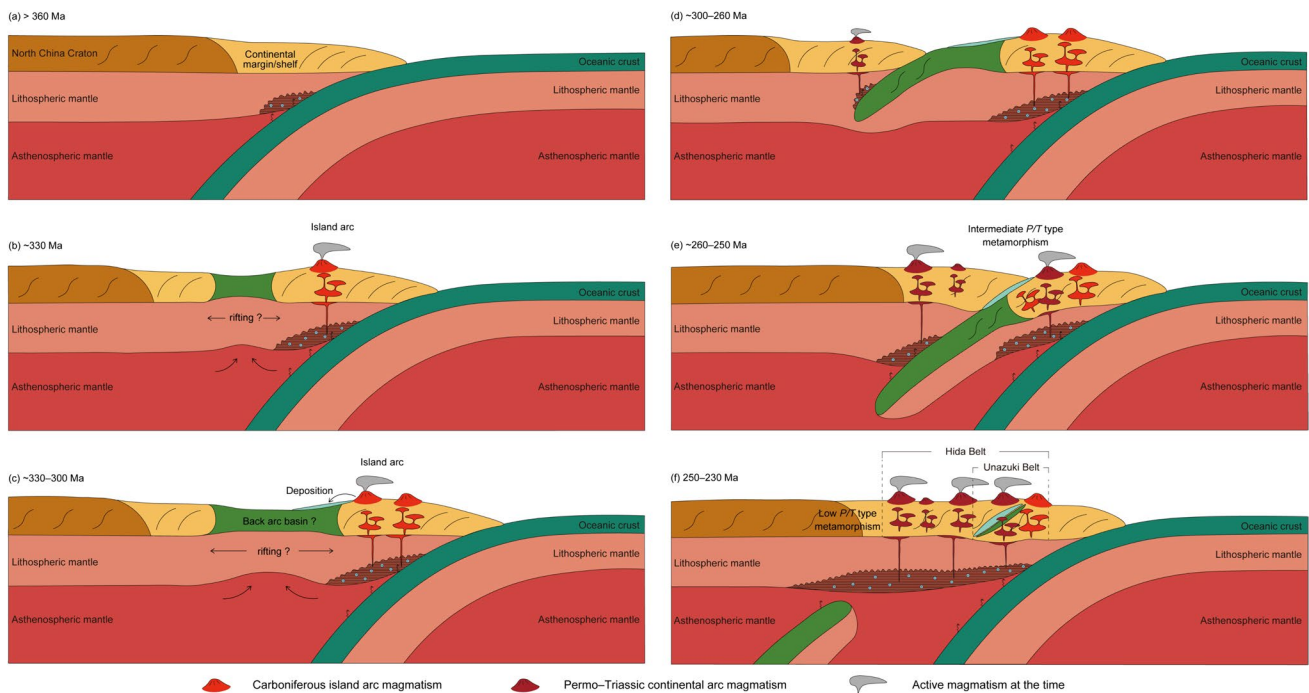
Fig. 15 Tectonic evolutional models of the Hida Belt, including the Unazuki Belt, from the Carboniferous to Triassic. **a** Subduction stage before ~360 Ma, forming the metasomatized lithospheric mantle beneath the East Asian continental margin. **b** Carboniferous island arc magmatism at ~330 Ma, with rifting on the East Asian continental margin. **c** Continuous Carboniferous island arc magmatism and deposition of the protolith of the Unazuki schists in the rifted basin probably the back-arc basin, during ~330–300 Ma. **d** Initiation of the subduction of the oceanic crust of the rifted back-arc basin during ~300–260 Ma with minor arc magmatism. **e** Collision between the East Asian continental margin and the Carboniferous island arc due to the closure of the rifted back-arc basin causing intermediate-*P/T*-type metamorphism for the Unazuki schists with the activation of continental arc magmatism during ~260–250 Ma. **f** Continuous continental arc magmatism in the Hida Belt, including the Unazuki Belt, until ~230 Ma

was formed not at the typical East Asian continental craton but at the juvenile continental margin, which formed from depleted mantle materials and/or their crustal derivatives and was separated from the continental craton (Fig. 15b). During ~330–300 Ma, protoliths of the metasedimentary rocks of the Unazuki Belt, including Late Carboniferous limestone (Hiroi et al. 1978), were deposited in the back-arc side, which possibly formed by the rifting of thin and juvenile continental margin rocks and was located next to the island arc, without input of cratonic materials from the East Asian continent (Fig. 15c). During the Permian period, the rifted basin probably the back-arc basin started to close with the subduction under the continental margin (Fig. 15d), possibly during ~300–260 Ma. At ~260–250 Ma, deposition continued with the input of cratonic materials (Fig. 15e). During this time, the Carboniferous island arc collided with the East Asian continental margin, resulting in a medium *P/T*-type metamorphism in the Unazuki Belt (Fig. 15e). After the collision of island arc and continental margin, subduction continued, and continental arc magmatism occurred in the Hida Belt, including the Unazuki Belt, until ~230 Ma with the melting of juvenile crust (Fig. 15f) as evidenced by the age of rhyolite magmatism (~250 Ma; Fig. 7c) with

positive $\varepsilon_{Hf}(t)$ values of zircon grains (Fig. 9). The island arc-continent collision due to the closure of the back-arc basin has also been proposed for the Permian Maizuru Belt, Southwest Japan (Suda et al. 2014; Mavoungou et al. 2022), and medium *P/T*-type metamorphism has been reported due to this collision process (Osozawa et al. 2004).

The occurrences of the Carboniferous subduction in the Hida Belt, including the Unazuki Belt, indicate that the Hida Belt had formed not at the southern and eastern margin of the SCC where the Carboniferous subduction is absent, but in the northeastern margin of the NCC, including the eastern margin of the northern Korean Peninsula, where the continuous subduction from Carboniferous to Permian is expected to have occurred (Song et al. 2015; Jeong and Oh 2021; Zhang et al. 2021). In the eastern part of the northern margin of the NCC, two pulses of subduction related magmatic activities occurred at 500–410 Ma and 360–220 Ma, with a magmatic hiatus between them (Song et al. 2015). The spatial–temporal distribution of the ophiolites and subduction-related igneous rocks indicate the double-side subduction toward the two continental margins viz., the northern margin of the NCC and the southern margin of the eastern CAOB (also called as Songlia Block) in the convergence

tectonic setting. Those two continental blocks collided at ~230–220 Ma, resulted in the formation of Xing'an-Inner Mongolia collision belt between them with a closure of the Paleo-Asian Ocean. In the whole belt, typical evidence of continental collision and Himalayan-style mountain building are absent, which suggests that the Xing'an-Inner Mongolia collision belt experienced "Appalachian-type" soft collision (Song et al. 2015). In the northern part of the eastern margin of the NCC including the northeastern Korean Peninsula, there was also Permian to Triassic igneous activities related to the subduction of the Paleo-Pacific plate (Ma et al. 2017; Zhang et al. 2021). The tectonic evolution of the northeastern margin of the NCC described above is well correlated to that of the Hida Belt including the Unazuki Belt.

The Jiamusi-Khanka Block is located to the east of the CAOB and the Mudanjiang Ocean situated between them during the Paleozoic. At least from the Permian, the Jiamusi-Khanka Block had approached to the eastern margin of the CAOB with subduction of oceanic crust under both sides (toward the eastern margin of the CAOB and the western margin of the Jiamusi-Khanka Block) and finally, the collision between the two blocks occurred, forming the Jilin-Heilongjiang Belt during 210–180 Ma (Yang et al. 2017; Zhou and Li 2017; Li et al. 2023). During 299–180 Ma, the subduction-accretion system formed along the eastern margin of the Jiamusi-Khanka Block due to the subduction of the Paleo-Pacific plate (Yang et al. 2015; Li et al. 2023). Due to the collision along the Jilin-Heilongjiang Belt, the subduction zone along the eastern margin of the Jiamusi-Khanka Block was connected to the subduction zone along the eastern margin of the NCC, resulted in the formation of the continuous subduction zone along the eastern margin of NE Asia where the Paleo-Pacific plate was subducted. The subduction along the eastern margin of the Jiamusi-Khanka Block continued until the Early Cretaceous at ~137–130 Ma (Li et al. 2023). The Hida Belt was also correlated with the subduction complex in the eastern margin of the Jiamusi-Khanka Block in previous studies (Zhao et al. 2013). However, during Carboniferous–Triassic time, the Jiamusi-Khanka Block occurred as a separated block that was not connected to the eastern margin of the NCC as discussed above. Although the Carboniferous detrital zircon grains constitute one of the major populations of the Permian Formations in the Jiamusi-Khanka Block (Xu et al. 2022), it is uncertain whether the mid-Carboniferous igneous activities occurred in the Jiamusi-Khanka Block or not due to the absence of the direct evidence such as the mid-Carboniferous arc magmatism. Therefore, it is difficult to correlate the Hida Belt with the Jiamusi-Khanka Block.

The Paleozoic tectono-thermal activity in the Korean Peninsula is not fully understood due to limited igneous activity, except for Permian arc magmatism (e.g., Yi et al. 2012; Choi et al. 2021). In the Pyeongan Supergroup of the Taebaeksan

Basin in the Korean Peninsula, Carboniferous detrital zircon grains of ~340–300 Ma were reported as a major population together with the ~1.9–1.8 Ga detrital zircon grains from Late Carboniferous to Early Permian strata (Kim et al. 2012, 2017, 2020), and Kim et al. (2012) suggested ~322–320 Ma arc origin igneous rocks as a source of the detrital zircon grains. Nevertheless, the source of the Carboniferous detrital zircon grains is unclear owing to the lack of reports of Carboniferous magmatism in the Korean Peninsula; therefore, Kim et al. (2012, 2017, 2020) suggested that the Hida Belt is a potential source of Carboniferous detrital zircon grains; however, certain Carboniferous magmatism in the Hida Belt has been unclear in the previous research reports. This problem can be solved through this study with newly identified Carboniferous island arc magmatism in the Unazuki Belt of the Hida Belt which can be a potential candidate for the source of the Carboniferous detrital zircon grains in the Pyeongan Supergroup of the Taebaeksan Basin. Moreover, paleocurrent analysis, in which the sediments in the Carboniferous Pyeongan Supergroup are suggested to have derived from the east or southeast (Lee and Lim 1995), further supports the source of the Carboniferous crustal materials from the Carboniferous island arc including the Unazuki Belt.

In the Hida Belt, the Hida Older and Younger Granites actively intruded during ~260–230 Ma and ~200–180 Ma, respectively, with a magmatic hiatus during ~230–200 Ma (Fig. 3). They were formed commonly under an arc tectonic setting (Cho et al. 2021; Yamada et al. 2021; Kawaguchi et al. 2023b). However, it is not clear why the magmatic hiatus occurred. On the other hand, the ~230–215 Ma igneous rocks were found in the Korean Peninsula and those were not formed under the typical arc tectonic setting but under the extension-related tectonic setting caused by slab roll-back (Lee et al. 2021; Kawaguchi et al. 2023a). In the Korean Peninsula, 230–215 Ma extension-related magmatism was followed by a magmatic hiatus from 215–200 Ma, suggesting that there was a transition in the tectonic environment from extension to compression during the magmatic hiatus. Following the consideration that the Korean Peninsula and Hida Belt were located along the continuous subduction zone during the Triassic (Kawaguchi et al. 2023a), slab roll-back may be one possible reason for the magmatic hiatus in the Hida Belt, but more studies will be needed to confirm this possibility.

Conclusions

1. In the Unazuki Belt, felsic plutonism and intermediate volcanism occurred at 328.2 ± 4.4 Ma and 332.8 ± 2.2 Ma, respectively, in an arc tectonic setting. The metasedimentary rocks of the Unazuki Belt yield the youngest detrital zircon grains of ~298 Ma

and ~ 305 Ma and have only Carboniferous single peaks without any Precambrian zircon. However, the meta-sedimentary rock of the Unazuki Belt with the youngest detrital zircon age of ~ 252 Ma has ~ 20% Precambrian zircon grains ranging in age from the Archean to Paleoproterozoic.

2. In the Unazuki Belt, the $\varepsilon_{Hf}(t)$ values of detrital zircon grains older than 300 Ma and those of ~ 330 Ma magmatic rocks are positive ($+6 \sim +18$), whereas the $\varepsilon_{Hf}(t)$ values for detrital zircon grains with ages between 280 and 250 Ma show a wide range between $+16$ and -23. These data indicate that in the Unazuki Belt, igneous zircon grains older than 300 Ma formed from juvenile sources, such as the depleted mantle and/or its crustal derivatives, but igneous zircon grains younger than 280 Ma formed from both matured and juvenile sources.

3. The igneous and sedimentary rocks in the Unazuki Belt formed in an island arc tectonic setting between ~ 330 Ma and ~ 300 Ma but in a continental arc tectonic setting at ~ 252 Ma. The collision between the island arc and continental margin may have occurred between 252 and 250 Ma, causing intermediate-*P/T* metamorphism in the Unazuki Belt.

4. The Carboniferous island arc igneous activity in the Hida Belt, including the Unazuki Belt, indicates that the Hida Belt had formed not in the southern margin of the SCC but in the eastern margin of the northern NCC, including the eastern margin of the northern Korean Peninsula.

Data availability All used data are available in the manuscript and the supplementary data.

Declarations

Conflict of interest The authors declare that they have no known competing financial interests or personal relationships that could have appeared to influence the work reported in this paper.

References

Arakawa Y (1984) Rb-Sr ages of the gneiss and metamorphosed intrusive rocks of the Hida metamorphic belt in the Urushiyama area, Gifu Prefecture, central Japan. J Japan Assoc Min Petr Econ Geol 11:431–442. https://doi.org/10.2465/ganko1941.79.431

Arakawa Y, Saito Y, Amakawa H (2000) Crustal development of the Hida belt, Japan: Evidence from Nd–Sr isotopic and chemical characteristics of igneous and metamorphic rocks. Tectonophysics 328:283–204. https://doi.org/10.1016/S0040-1951(00)00183-9

Bhatia MR (1983) Plate tectonics and geochemical composition of sandstones. J Geol 91:611–627. https://doi.org/10.1086/628815

Bhatia MR, Crook KAW (1986) Trace element characteristics of graywackes and tectonic setting discrimination of sedimentary basins. Contrib Mineral Petrol 92:181–193. https://doi.org/10.1007/BF00375292

Blichert-Toft J, Albarède F (1997) The Lu-Hf isotope geochemistry of chondrites and the evolution of the mantle-crust system. Earth Planet Sci Lett 148:243–258. https://doi.org/10.1016/S0012-821X(97)00040-X

Cho DL, Lee TH, Takahashi Y, Kato T, Yi K, Lee S, Cheong ACS (2021) Zircon U-Pb geochronology and Hf isotope geochemistry of magmatic and metamorphic rocks from the Hida Belt, southwest Japan. Geosci Front 12:101145. https://doi.org/10.1016/j.gsf.2021.101145

Choi HO, Choi SH, Kim SS (2021) Zircon U-Pb geochronology and Sr–Nd–Pb–Hf isotope geochemistry for Permian-Early Triassic arc-related magmatism in Pohang, Jangsari, and Yeongdeok, southeastern Korean Peninsula. Lithos. https://doi.org/10.1016/j.lithos.2020.105930

Defant MJ, Richerson PM, De Boer JZ, Stewart RH, Maury RC, Bellon H, Drummond MS, Feigenson MD, Jackson TE (1991) Dacite genesis via both slab melting and differentiation: Petrogenesis of La Yeguada Volcanic Complex, Panama. J Petrol 32:1101–1142. https://doi.org/10.1093/petrology/32.6.1101

Dunkley DJ, Suzuki K, Hokada T, Kusiak MA (2008) Contrasting ages between isotopic chronometers in granulites: monazite dating and metamorphism in the Higo Complex, Japan. Gondwana Res 14:624–643. https://doi.org/10.1016/j.gr.2008.02.003

Ehiro M, Tsujimori T, Tsukada K, Nuramkhaan M (2016) Paleozoic basement and associated cover. In: Moreno T, Wallis S, Kojima T, Gibbons W (eds) The geology of Japan. The Geological Society of London, London, pp 25–60

Ernst WG, Cao R, Jiang J (1988) Reconnaissance study of precambrian metamorphic rocks, northeastern sino-Korean shield, people's republic of China. Geol Soc Am Bull 100:692–701

Fujii M, Hayasaka Y, Terada K (2008) SHRIMP zircon and EPMA monazite dating of granitic rocks from the maizuru terrane, southwest Japan: correlation with east asian paleozoic terranes and geological implications. Island Arc 17:322–341. https://doi.org/10.1111/j.1440-1738.2008.00623.x

Goolaerts A, Mattielli N, Jong JD, Weis D, Scoates JS (2004) Hf and Lu isotopic reference values for the zircon standard 91500 by MC-ICP-MS. Chem Geol 206:1–9. https://doi.org/10.1016/j.chemgeo.2004.01.008

Griffin WL, Wang X, Jackson SE, Pearson NJ, O'Reilly SY, Xu X, Zhou X (2002) Zircon chemistry and magma mixing, SE China: in situ analysis of Hf isotopes, Tonglu and Pingtan igneous complexes. Lithos 61:237–269. https://doi.org/10.1016/S0024-4937(02)00082-8

Harmon RS, Barreiro BA (1984) Andean Magmatism: Chemical and Isotopic Constraints. Shiva Publishing Limited, UK

Harris NB, Pearce JA, Tindle AG (1986) Geochemical characteristics of collision-zone magmatism. Geol Soc Spec Publ 19:67–81. https://doi.org/10.1144/GSL.SP.1986.019.01.04

Hayasaka Y (1987) Study on the late paleozoic-early mesozoic tectonic development of western half of the inner zone of Southwest Japan. Geol Rep Hiroshima Univ 27:119–204

Hiroi Y (1978) Geology of the Unazuki district in the hida metamorphic terrain, central Japan. J Geol Soc Japan 84:521–530. https://doi.org/10.5575/geosoc.84.521

Hiroi Y (1980) Petrography of the unazuki pelitic schist, hida terrane, Central Japan. Bull Faculty Educ Kanazawa Univ 28:69–87

Hiroi Y (1981) Subdivision of the hida metamorphic complex, central Japan, and its bearing on the geology of the far east in pre-sea of Japan time. Tectonophysics 76:317–333. https://doi.org/10.1016/0040-1951(81)90103-7

Hiroi Y (1983) Progressive metamorphism of the unazuki pelitic schists in the hida terrane, Central Japan. Contrib Mineral Petrol 82:334–350. https://doi.org/10.1007/BF00399711

Hiroi Y (1984) Petrography of unazuki pelitic schists, hida terrane, Central Japan (part 2). Bull Faculty Educ Kanazawa Univ 33:69–87

Hiroi Y, Fuji N, Okimura Y (1978) new fossil discovery from the hida metamorphic rocks in the unazuki area, Central Japan. Proc Jpn Acad Ser B 54:268–271. https://doi.org/10.2183/pjab.54.268

Horie K, Yamashita M, Hayasaka Y, Katoh Y, Tsutsumi Y, Katsube A, Hidaka H, Kim H, Cho M (2010) Eoarchean-paleoproterozoic zircon inheritance in japanese permo-triassic granites (unazuki area, hida metamorphic complex): unearthing more old crust and identifying source terranes. Precambrian Res 183:145–157. https://doi.org/10.1016/j.precamres.2010.06.014

Horie K, Takehara M, Suda Y, Hidaka H (2013) Potential mesozoic reference zircon from the unazuki plutonic complex: geochronological and geochemical characterization. Island Arc 22:292–305. https://doi.org/10.1111/iar.12031

Horie K, Tsutsumi Y, Takehara M, Hidaka H (2018) Timing and duration of regional metamorphism in the kagasawa and unazuki areas, hida metamorphic complex, southwest Japan. Chem Geol 484:148–167. https://doi.org/10.1016/j.chemgeo.2017.12.016

Hu ZC, Liu YS, Gao S, Liu W, Yang L, Zhang W, Tong X, Lin L, Zong KQ, Li M, Chen H, Zhou L (2012) Improved in situ Hf isotope ratio analysis of zircon using newly designed X skimmer cone and Jet sample cone in combination with the addition of nitrogen by laser ablation multiple collector ICP-MS. J Anal Spectrom 27:1391–1399. https://doi.org/10.1039/C2JA30078H

Ishioka K (1949) Staurolite and kyanite near unazuki in the lower kurobe-gawa area. J Geol Soc Jpn 55:156 ((**In Japanese**))

Ishioka K, Suwa K (1954) Fabric of hornblende in a schistose amphibolite from the Kurobe-Gawa area, central Japan. J Earth Sci Nagoya Univ 2:191–199

Ishioka K, Suwa K (1956) Metasomatic development of staurolite schist from rhyolite in the kurobe-gawa area, central Japan. Preliminary Rept J Earth Sci Nagoya Univ 4:123–140

Ishiwatari A, Tsujimori T (2003) Paleozoic ophiolites and blueschists in Japan and Russian Primorye in the tectonic framework of East Asia: a synthesis. Island Arc 12:190–206. https://doi.org/10.1046/j.1440-1738.2003.00390.x

Isozaki Y (1997) Contrasting two types of orogen in permo-triassic Japan: accretionary versus collisional. Island Arc 6:2–24

Isozaki Y, Aoki K, Nakama T, Yanai S (2010) New insight into a subduction-related orogen: a reappraisal of the geotectonic framework and evolution of the Japanese Islands. Gondwana Res 18:82–105. https://doi.org/10.1016/j.gr.2010.02.015

Jeong JW, Oh CW (2021) A comprehensive review of previous studies on permo-triassic metamorphic and igneous activities, and tectonic evolution in the korean peninsula. J Geol Soc Korea 57:545–564

Kang MS, Oh CW, Lee BC, Lee BY (2023) The tectonic evolution from the archean to triassic in the north central gyeonggi massif (hongcheon-chuncheon areas) in the Korean peninsula, and its application to the tectonic evolution of the North China craton. Earth Sci Rev 247:104605. https://doi.org/10.1016/j.earscirev.2023.104605

Kano T (1990) Granitic rocks in the Hida complex, central Japan. Min Geol 40:397–413

Kawaguchi K, Hayasaka Y, Shibata T, Komatsu M, Kimura K, Das K (2020) Discovery of paleozoic rocks at northern margin of sambagawa terrane, eastern kyushu, japan: petrogenesis, u-pb geochronology and its tectonic implication. Geosci Front 11:1441–1459. https://doi.org/10.1016/j.gsf.2020.01.001

Kawaguchi K, Oh CW, Jeong JW (2023a) Geochemistry, zircon u-pb ages and lu–hf isotopes of triassic plutons in the eastern gyeonggi massif, korean peninsula: magma genesis and geodynamic implications for East Asia. Lithos 436–437:106955. https://doi.org/10.1016/j.lithos.2022.106955

Kawaguchi K, Oh CW, Jeong JW, Furusho M, Shibata S, Hayasaka Y (2023b) Zircon U-Pb ages and Lu–Hf isotopes of the Jurassic Granites on the east coast of the Korean Peninsula and Southwest Japan: Petrogenesis and tectonic correlation between the Korean Peninsula and Japanese Islands. Gondwana Res 117:56–85. https://doi.org/10.1016/j.gr.2023.01.005

Kim HS, Ree JH, Kim J (2012) Tectonometamorphic evolution of the permo-triassic songrim (indosinian) orogeny: evidence from the late paleozoic pyeongan supergroup in the northeastern taebaeksan basin, South Korea. Int J Earth Sci 101:483–498. https://doi.org/10.1007/s00531-011-0683-x

Kim MG, Lee YI, Choi T (2017) The tectonic setting of the eastern margin of the sino-korean block inferred from detrital zircon u-pb age and nd isotope composition of the pyeongan supergroup (upper palaeozoic – lower triassic), Korea. Geol Mag 156:471–484. https://doi.org/10.1017/S0016756817000899

Kim KG, Lee YI, Choi T (2020) Tectonic setting of the eastern margin of the sino-korean block in the pennsylvanian: constraints from detrital zircon ages. Minerals 10:527. https://doi.org/10.3390/min10060527

Kimura K, Hayasaka Y (2019) Zircon u-pb age and nd isotope geochemistry of latest neoproterozoic to early paleozoic oeyama ophiolite: evidence for oldest morb-type oceanic crust in

japanese accretionary system and its tectonic implications. Lithos 342–343:345–360. https://doi.org/10.1016/j.lithos.2019.06.001

Kimura K, Hayasaka Y, Shibata T, Kawaguchi K, Fujiwara H (2019) Discovery of paleoproterozoic 1.85 ga granitoid bodies from the maizuru terrane in the tsuwano area, shimane prefecture, southwest japan and its geologic implications. J Geol Soc Japan 125:153–165. https://doi.org/10.5575/geosoc.2018.0050

Kimura K, Hayasaka Y, Yamashita J, Shibata T, Kawaguchi K, Fujiwara H, Das K (2021) Antiquity and tectonic lineage of Japanese Islands: new discovery of archean-paleoproterozoic Complex. Earth Planet Sci Lett 565:116926. https://doi.org/10.1016/j.epsl.2021.116926

Kobayashi T (1941) The sakawa orogenic cycle and its bearing on the origin of the Japanese Islands. J Fac Sci Imp. Univ Tokyo Sec II 5:219–578

Koizumi S, Otoh S (2019) The Triassic plutonic and metamorphic rocks in the Saragawa-Bandojima area, Katsuyama City, Fukui Prefecture, central Japan. Katsuyama City Geopark Academic Research Project, Academic Research Reports, pp 18 (in Japanese with English abstract). https://www.city.katsuyama.fukui.jp/geopark/about/pdf/2019koizumi.pdf

Kojima S, Hayasaka Y, Hiroi Y, Matsuoka A, Sano H, Sugamori Y, Suzuki N, Takemura S, Tsujimori T, Uchino T (2016) Pre-cretaceous accretionary complexes. In: Moreno T, Wallis S, Kojima T, Gibbons W (eds) The geology of Japan. The Geological Society of London, London, pp 61–100

Komatsu M, Ujihara M, Chihara K (1985) Pre-Tertiary basement structure in the inner zone of honshu and the North fossa magna region. Sci Rep Niigata Univ Ser E Geol Mineral 5:133–148

Lee YI, Lim C (1995) Provenance and variance of the Carboniferous Manhang sandstones, central eastern Korea. J Geol Soc Korea 31:637–652

Lee BC, Oh CW, Yi K (2016) Geochemistry, zircon u-pb ages, and hf isotopic compositions of precambrian gneisses in the wonjujechon area of the southern gyeonggi massif: implications for the precambrian tectonic evolution of Korea and northeast Asia. Precambrian Res 283:169–189. https://doi.org/10.1016/j.precamres.2016.07.014

Lee BC, Jo HJ, Lee SH, Jeong YJ (2021) Geochronology and petrogenesis of the late triassic a-type granitoids in the yeongnam massif and its implication for late triassic geodynamics of northeast Asia. Lithos 386–387:106018. https://doi.org/10.1016/j.lithos.2021.106018

Li GY, Zhou JB, Li L (2023) The Jiamusi block: a hinge of the tectonic transition from the paleo-asian ocean to the paleo-pacific ocean regimes. Earth Sci Rev 236:104279. https://doi.org/10.1016/j.earscirev.2022.104279

Liu YS, Hu ZC, Gao S, Günther D, Xu J, Gao CG, Chen HH (2008) In situ analysis of major and trace elements of anhydrous minerals by LA-ICP-MS without applying an internal standard. Chem Geol 257:34–43. https://doi.org/10.1016/j.chemgeo.2008.08.004

Liu YS, Gao S, Hu ZC, Gao CG, Zong KQ, Wang DB (2010) Continental and oceanic crust recycling-induced melt-peridotite interactions in the Trans-North China Orogen: U-Pb dating, Hf isotopes and trace elements in zircons from mantle xenoliths. J Petrol 51:537–571. https://doi.org/10.1093/petrology/egp082

Ludwig KR (2003) User's manual for Isoplot 3.00. Berkeley Geochronol Center Special Publ 4:1–71

Ma XH, Zhu WP, Zhou ZH, Qiao SL (2017) Transformatin from paloeasian ocean closure to paleo-pacific subduction: new constraints from granitoids in the eastern jilin-heilongjiang belt, NE China. J Asian Earth Sci 144:261–286

Maruyama S, Liou JG, Seno T (1989) Mesozoic and Cenozoic evolution of Asia. In: Zvi BA (ed) The evolution of the Pacific Ocean margins. Oxford University, Oxford, pp 75–99

Matcalfe I (2006) Palaeozoic and Mesozoic tectonic evolution and palaeogeography of East Asian crustal fragments: The Korean Peninsula in context. Gondwana Res 9:24–46

Mavoungou LN, Das K, Kawaguchi K, Hayasaka Y, Shibata T (2022) Back-arc basin closure at the east asian margin during permotriassic boundary: evidence from geochemistry and u-pb zircon data of sedimentary breccia from maizuru terrane. Southwest Japan Geosyst Geoenviron 1:100080. https://doi.org/10.1016/j.geogeo.2022.100080

Middlemost EA (1994) Naming materials in the magma/igneous rock system. Earth Sci Rev 37:215–224. https://doi.org/10.1016/0012-8252(94)90029-9

Mizutani S, Hattori I (1983) Hida and Mino: tectonostratigraphic terranes in central Japan. In: Hashimoto M, Uyeda S (eds) Accretion Tectonics in the Circum-Pacific Regions. Terra Science, Tokyo, pp 169–178

Oh CW (2006) A new concept on tectonic correlation between Korea, China and Japan: Histories from the late proterozoic to cretaceous. Gondwana Res 9:47–61. https://doi.org/10.1016/j.gr.2005.06.001

Oh CW, Kusky T (2007) the late permian to triassic hongseong-odesan collision belt in South Korea, and its tectonic correlation with China and Japan. Int Geol Rev 49:636–657. https://doi.org/10.2747/0020-6814.49.7.636

Osanai Y, Owada M, Kamei A, Hamamoto T, Kagami H, Toyoshima T, Nakano N, Nam TN (2006) The higo metamorphic complex in Kyushu, Japan as the fragment of permo-triassic metamorphic complexes in East Asia. Gondwana Res 9:152–166. https://doi.org/10.1016/j.gr.2005.06.008

Osanai Y, Yoshimoto A, Nakano N, Adachi T, Kitano I, Yonemura K, Sasaki J, Tsuchiya N, Ishizuka H (2014) LA-ICP-MS zircon U-Pb geochronology of Paleozoic granitic rocks and related igneous rocks from the Kurosegawa tectonic belt in Kyushu, Southwest Japan. Jpn Mag Mineral Petrol Sci 43:71–99. https://doi.org/10.2465/gkk.131126

Osozawa S, Takeuchi H, Koitabashi T (2004) Formation of the Yakuno ophiolite; accretionary subduction under medium-pressure-type metamorphic conditions. Tectonophysics 393:197–219. https://doi.org/10.1016/j.tecto.2004.07.033

Otofuji Y (1996) Large tectonic movement of the Japan Arc in late Cenozoic times inferred from paleomagnetism: review and synthesis. Island Arc 5:229–249. https://doi.org/10.1111/j.1440-1738.1996.tb00029.x

Otofuji Y, Matsuda T (1984) Timing of rotational motion of Southwest Japan inferred from paleomagnetism. Earth Planet Sci Lett 70:373–382. https://doi.org/10.1016/0012-821X(84)90021-9

Pearce JA, Harris NB, Tindle AG (1984) Trace element discrimination diagrams for the tectonic interpretation of granitic rocks. J Petrol 25:956–983. https://doi.org/10.1093/petrology/25.4.956

Peccerillo A, Taylor SR (1976) Geochemistry of eocene calc-alkaline volcanic rocks from the kastamonu area, Northern Turkey. Contrib Miner Petrol 58:63–81. https://doi.org/10.1007/BF00384745

Polat A, Hofmann AW, Rosing MT (2002) Boninite-like volcanic rocks in the 3.7– 3.8 Ga Isua greenstone belt, West Greenland: geochemical evidence for intra- oceanic subduction zone processes in the early earth. Chem Geol 184:231–254. https://doi.org/10.1016/S0009-2541(01)00363-1

Sakoda M, Kano T, Fanning CM, Sakaguchi T (2006) SHRIMP U-Pb zircon age of the inishi migmatite around the kamioka mining area, hida metamorphic complex, Central Japan. Resour Geol 56:17–26. https://doi.org/10.1111/j.1751-3928.2006.tb00264.x

Sawada H, Niki S, Nagata M, Hirata T (2022) Zircon U-Pb–Hf isotopic and trace element analyses for oceanic mafic crustal rock of the neoproterozoic-early paleozoic oeyama ophiolite unit and implication for subduction initiation of proto-Japan arc. Minerals 12:107. https://doi.org/10.3390/min12010107

Shibata K, Nozawa T (1986) Late Precambrian ages for granitic rocks intruding the Hida Metamorphic Rocks. Bull Geol Surv Japan 37:43–51

Shibata K, Nozawa T, Wanless RK (1970) Rb-Sr geochronology of the Hida metamorphic belt, Japan. Can J Earth Sci 7:1383–1401

Shibata K, Kano T, Asano M (1989) Isotopic ages of the gray granite from the upper kubusu river area, hida mountains. J Mineral Petrol Econ Geol 84:243–251. https://doi.org/10.2465/ganko.84.243

Sláma J, Košler J, Condon DJ, Crowley JL, Gerdes A, Hanchar JM, Horstwood MSA, Morris GA, Nasdala L, Norberg N, Schaltegger U, Schoene B, Tubrett MN, Whitehouse MJ (2008) Plešovice zircon — a new natural reference material for U-Pb and Hf isotopic microanalysis. Chem Geol 249:1–35. https://doi.org/10.1016/j.chemgeo.2007.11.005

Söderlund U, Patchett JP, Vervoort JD, Isachsen CE (2004) The ^{176}Lu decay constant determined by Lu–Hf and U-Pb isotope systematics of Precambrian mafic intrusions. Earth Planet Sci Lett 219:311–324. https://doi.org/10.1016/S0012-821X(04)00012-3

Sohma T, Kunugiza K, Terabayashi M (1990) Hida metamorphic belt. In: Excursion Guidebook of the 96th Annual Meeting of Geol Soc Japan, pp 27–53 (in Japanese with English abstract).

Sohma T, Kunugiza K (1993) The formation of the Hida nappe and the tectonics of Mesozoic sediments: The tectonic evolution of the Hida region Central Japan. J Geol Soc Japan 42:1–20

Song S, Wan MM, Xu X, Wang C, Niu Y, Allen MB, Su L (2015) Ophiolites in the Xing'an-Inner Mongolia accretionary belt of the CAOB: Implications for two cycles of seafloor spreading and accretionary orogenic events. Tectonics 34:2221–2248

Stephen AW, Robert LW (2012) Certificate of Analysis Standard Reference Material 610. National Institute of Standard & Technology Gaithersburg, pp 4.

Suda Y, Hayasaka Y, Kimura K (2014) Crustal evolution of a Paleozoic intra-oceanic Island-Arc-back-arc basin system constrained by the geochemistry and geochronology of the Yakuno Ophiolite, Southwest Japan. J Geolog Res, doi: https://doi.org/10.1155/2014/652484

Sun SS, Mcdonough WF (1989) Chemical and isotopic systematics of oceanic basalts: implications for mantle composition and processes. Geol Soc Spec Publ 42:313–345. https://doi.org/10.1144/GSL.SP.1989.042.01.19

Suzuki K, Adachi M (1991) The chemical Th-U-total Pb isochron ages of zircon and monazite from the Gray Granite of the Hida terrane, Japan. Jour Earth Sci Nagoya Univ 38:11–37

Suzuki K, Adachi M (1994) Middle Precambrian detrital monazite and zircon from the Hida gneiss on Oki-Dogo Island, Japan: their origin and implications for the correlation of basement gneiss of Southwest Japan and Korea. Tectonophysics 235:277–292

Suzuki M, Nakazawa S, Osakabe T (1989) Tectonic development of the Hida Belt – with special reference to its metamorphic history and late Carboniferous to Triassic orogenies–. Mem Geol Soc Jpn 33:1–100 ((**In Japanese with English abstract**))

Takahashi Y, Cho DL, Kee WS (2010) Timing of mylonitization in the Funatsu Shear Zone within Hida Belt of southwest Japan: Implications for correlation with the shear zones around the Ogcheon Belt in the Korean Peninsula. Gondwana Res 17:102–115. https://doi.org/10.1016/j.gr.2009.04.008

Takahashi Y, Cho DL, Mao J, Zhao X, Yi K (2018) SHRIMP U-Pb zircon ages of the hida metamorphic and plutonic rocks, Japan: implications for late paleozoic to mesozoic tectonics around the Korean peninsula. Island Arc 27:e12220. https://doi.org/10.1111/iar.12220

Takehara M, Horie K (2019) U-Pb zircon geochronology of the Hida gneiss and granites in the Kamioka area. Hida Belt Island Arc 28:e12303. https://doi.org/10.1111/iar.12303

Takeuchi M, Shibata K, Jia S, Yamamoto K (2019) U-Pb zircon ages of granitic rocks from kagasawa, hida mountains. J Geol Soc Japan 125:453–459. https://doi.org/10.5575/geosoc.2019.0009

Takeuchi M, Jia S, Shimura Y (2021) Zircon U-Pb ages on plutonic rocks in the eastern area of 1:200,000 quadrangle, Toyama, central Japan. Bull Geol Surv Japan 72:41–64. https://doi.org/10.9795/bullgsj.72.41

Takeuchi M, Furukawa R, Nagamori H, Oikawa T (2017) Geology of the Tomari District. Quadrangle Series, 1:50,000, Geological Survey of Japan, AIST, pp 121 (in Japanese with English abstract).

Wakita K (2013) Geology and tectonics of Japanese islands: a review – the key to understanding the geology of Asia. J Asian Earth Sci 72:75–87. https://doi.org/10.1016/j.jseaes.2012.04.014

Wakita K, Nakagawa T, Sakata M, Tanaka N, Oyama N (2021) Phanerozoic accretionary history of Japan and the western Pacific margin. Geol Mag 158:13–29. https://doi.org/10.1017/S0016756818000742

Wang X, Oh CW, Lee BC, Liu F (2020a) Paleoproterozoic postcollisional metamorphic and igneous activities in the Jinan area of the Jiao-Liao-Ji Belt in the North China Craton and their tectonic implications. Precambrian Res 346:105793. https://doi.org/10.1016/j.precamres.2020.105793

Wang X, Oh CW, Peng P, Zhai M, Wang X, Lee BY (2020b) Distribution pattern of age and geochemistry of 2.18–2.14 Ga I- and A-type granites and their implication for the tectonics of the Liao-Ji belt in the North China Craton. Lithos. https://doi.org/10.1016/j.lithos.2020.105518

Wiedenbeck M, Alle P, Corfu F, Griffin WL, Meier M, Oberli F, Quadt AV, Roddick JC, Spiegel W (1995) Three natural zircon standards for U-Th-Pb, Lu- Hf, trace element and REE analyses. Geostand Geoanalytical Res 19:1–23. https://doi.org/10.1111/j.1751-908X.1995.tb00147.x

Winter JD (2014) Subduction-Related Igneous Activity, Part II: Continental Arcs. In Winter JD (ed) Principles of Igneous and Metamorphic Petrology Second Edition, pp 369–394.

Woodhead JD, Hergt JM (2005) A preliminary appraisal of seven natural zircon reference materials for in situ Hf isotope determination. Geostand Geoanalytical Res 29:183–195. https://doi.org/10.1111/j.1751-908X.2005.tb00891.x

Xu ZJ, Sun NC, Zhou JB, Kong JT, Cheng RH, Li Z (2022) The early permian assembly of the jiamusi massif and khanka massif: evidence from sediment sources. Geological J 57:4325–4344. https://doi.org/10.1002/gj.4547

Yamada R, Sawada H, Aoyama S, Ouchi W, Niki S, Nagata M, Takahashi T, Hirata T (2021) Zircon U-Pb ages and whole–rock geochemistry from the Hida granites: implications for the geotectonic history and the origin of Mesozoic granites in the Hida belt, Japan. J Mineral Petrol Sci 116:61–66. https://doi.org/10.2465/jmps.201125

Yamaguchi M, Yanagi T (1968) The Rb-Sr ages of the so-called leptite, Unazuki. (Abstr.). J Geol Soc Japan 74:91

Yamaguchi M, Yanagi T (1970) Geochronology of some metamorphic rocks in Japan. Eclogae Geol Helv 64:371–388

Yang H, Ge WC, Zhao G, Yu J, Zhang Y (2015) Early permian-late triassic granitic magmatism in the jiamusi-khanka massif, eastern segment of the central asian orogenic belt and its implications. Gondwana Res 28:1509–1533. https://doi.org/10.1016/j.gr.2014.01.011

Yang H, Ge W, Dong Y, Bi J, Wang Z, Ji Z, Yang H, Ge WC, Dong Y, Bi JH, Wang ZH, Ji Z (2017) Record of permian-early triassic continental arc magmatism in the western margin of the jiamusi block, ne china: petrogenesis and implications for paleo-pacific subduction. Int J Earth Sci 106:1919–1942. https://doi.org/10.1007/s00531-016-1396-y

Yi K, Cheong CS, Kim J, Kim N, Jeong YJ, Cho M (2012) Late paleozoic to early mesozoic arc-related magmatism in southeastern Korea: SHRIMP zircon geochronology and geochemistry. Lithos 153:129–141. https://doi.org/10.1016/j.lithos.2012.02.007

Yoshida T, Taguchi T, Ueda H, Horie K, Satish-Kumar M (2020) Early carboniferous hp metamorphism in the Hida Gaien belt, Japan: implications for the palaeozoic tectonic history of proto-Japan. J Metamorph Geol 39:77–100. https://doi.org/10.1111/jmg.12564

Zhang YB, Zhai MG, Wu FY, Zhang XH, Li QL, Peng P, Zhao L, Zhou LG (2021) Review on the paleozoic -mesozoic granitoids and sedimentary rocks in North Korea. J Geol Soc Korea 57:523–544

Zhao X, Mao J, Ye H, Liu K, Takahashi Y (2013) New SHRIMP U-Pb zircon ages of granitic rocks in the Hida Belt, Japan: Implications for tectonic correlation with Jiamushi massif. Island Arc 22:508–521. https://doi.org/10.1111/iar.12045

Zhou JB, Li L (2017) The mesozoic accretionary complex in Northeast China: evidence for the accretion history of paleo-pacific subduction. J Asian Earth Sci 145:91–100. https://doi.org/10.1016/j.jseaes.2017.04.013

Zong K, Klemd R, Yuan Y, He Z, Guo J, Shi X, Liu Y, Hu Z, Zhang Z (2017) The assembly of rodinia: the correlation of early neoproterozoic (ca. 900 Ma) high-grade metamorphism and continental arc formation in the southern beishan orogen, southern central asian orogenic belt (caob). Precambrian Res 290:32–48. https://doi.org/10.1016/j.precamres.2016.12.010